Open-File Miscellaneous Investigation 21–02.0

GEOHYDROLOGIC AND WATER-QUALITY CHARACTERIZATION OF A FRACTURED-BEDROCK TEST HOLE IN AN AREA OF MARCELLUS SHALE GAS DEVELOPMENT, SULLIVAN COUNTY, PENNSYLVANIA

---

by Dennis W. Risser
John H. Williams
U.S. Geological Survey

Aaron D. Bierly
Pennsylvania Geological Survey

PENNSYLVANIA GEOLOGICAL SURVEY
FOURTH SERIES
HARRISBURG

Prepared in cooperation with the U.S. Geological Survey

2021

REPORT DISCLAIMER

No Warranty

This open-file report and accompanying documentation are provided "as is," and the user assumes the entire risk as to their quality and performance.

The Commonwealth of Pennsylvania makes no guarantee or warranty concerning the accuracy of information contained in the geographic data or accompanying documentation. The Commonwealth of Pennsylvania further makes no warranties, either expressed or implied, as to any other matter whatsoever, including, without limitation, the completeness or condition of the product, or its fitness for any particular purpose. The burden for determining fitness for use lies entirely with the user.

Although the text and map image have been processed successfully on a computer system at the Bureau Geological Survey, the Commonwealth of Pennsylvania makes no warranty, expressed or implied, regarding the use of the report or accompanying documentation on any other computer system, nor does the act of distribution constitute any such warranty.

Limitation of Liability

The user shall save the Commonwealth of Pennsylvania harmless from any suits, claims, or actions arising out of the use of or any defect in the open-file report or accompanying documentation.

The Commonwealth of Pennsylvania assumes no legal liability for the accuracy, completeness, or usefulness of the open-file report and accompanying documentation. In no event shall the Commonwealth of Pennsylvania have any liability whatsoever for payment of any consequential, incidental, indirect, special, or tort damages of any kind, including, but not limited to, any loss of profits arising out of use of or reliance on the geographic or geologic data.

Use and Access Constraints

Not for commercial resale.

This open-file report is not designed for use as a primary regulatory tool in permitting and siting decisions. It is public information and, as such, it may be used as a reference source and may be interpreted by organizations, agencies, units of government, or others based on needs; however, each user is responsible for the appropriate application of the data. Federal, state, or local regulatory bodies are not to reassign to the Bureau of Geological Survey any authority for the decisions they make using this report.

Endorsements

The use of trade, product, or firm names in this report is for descriptive purposes only and does not imply endorsement by the authors or their employers.

COMMONWEALTH OF PENNSYLVANIA
Tom Wolf, *Governor*
DEPARTMENT OF CONSERVATION AND NATURAL RESOURCES
Cindy Adams Dunn, *Secretary*
OFFICE OF CONSERVATION AND TECHNICAL SERVICES
Lauren Imgrund, *Deputy Secretary*
BUREAU OF TOPOGRAPHIC AND GEOLOGIC SURVEY
Gale C. Blackmer, *Director*

This report has been reviewed by staff of the Pennsylvania Geological Survey
and has undergone external peer review in accordance with
the fundamental science practices of the U.S. Geological Survey.

COVER

Drilling of the Laporte test hole and collection of rock cuttings, Sullivan County, Pa. Photography by Dennis Risser, U.S. Geological Survey.

FUNDING

This report was funded in part by the
USGS National Cooperative Geologic Mapping Program
under STATEMAP Award Number G12AC20270
and by the USGS Toxics Substances Hydrology Program

Instructions for obtaining the complete report can be found at
https://www.dcnr.pa.gov/Geology/PublicationsAndData

Suggested citation: Risser, D. W., Williams, J. H., and Bierly, A. D., 2021, Geohydrologic and water-quality characterization of a fractured-bedrock test hole in an area of Marcellus shale gas development, Sullivan County, Pennsylvania: Pennsylvania Geological Survey, 4th ser., Open-File Report OFMI 21–02.0, 56 p. plus appendices.

[BLANK PAGE]

CONTENTS

APPENDICES

(included as separate files)

FIGURES

TABLES

CONVERSION FACTORS

Multiply inch-pound units	by	To obtain SI units
	Length	
inch (in.)	25.4	millimeter (mm)
foot (ft)	0.3048	meter (m)
mile (mi)	1.609	kilometer (km)
	Area	
acre	0.004047	square kilometer (km^2)
square foot (ft^2)	0.09290	square meter (m^2)
square mile (mi^2)	2.590	square kilometer (km^2)
	Volume	
gallon (gal)	3.785	liter (L)
cubic foot (ft^3)	0.02832	cubic meter (m^3)
	Flow rate	
foot per second (ft/s)	0.3048	meter per second (m/s)
cubic foot per day (ft3/d)	0.02832	Cubic meter per day (m^3/d)
gallon per minute (gal/min)	0.06309	liter per second (L/s)
	Pressure	
atmosphere, standard (atm)	101.3	kilopascal (kPa)
inch of mercury at 60°F (inHg)	3.377	kilopascal (kPa)
pound per square inch (lb/in^2)	6.895	kilopascal (kPa)
	Radioactivity	
picocurie per liter (pCi/L)	0.037	becquerel per liter (Bq/L)
	Specific Capacity	
gallon per minute per foot [(gal/min)/ft]	0.2070	liter per second per meter [(L/s)/m]
	Transmissivity	
square foot per day (ft^2/d)	0.09290	square meter per day (m^2/d)

- Temperature in degrees Celsius (°C) may be converted to degrees Fahrenheit (°F) as follows: °F = (1.8×°C) + 32.
- Vertical coordinate information is referenced to the North American Vertical Datum of 1988 (NAVD 88).
- Horizontal coordinate information is referenced to the North American Datum of 1983 (NAD 83).
- Altitude, as used in this report, refers to distance above the vertical datum.
- Specific conductance is given in microsiemens per centimeter at 25 degrees Celsius (µS/cm at 25°C).
- Concentrations of chemical constituents in water are given in milligrams per liter (mg/L) or micrograms per liter (µg/L).

EXPLANATION OF STRATIGRAPHIC, BEDDING, FRACTURE, AND GEOPHYSICAL LOG HEADINGS

Depth	Depth, in feet below land surface (ft bls)
Age	Geologic age
Form	Stratigraphic formation
Gamma	Gamma radiation log, in counts per second (CPS)
Neutron Porosity	Neutron-porosity log, in fraction of total volume occupied by pores or voids (V/V)
Mag Suscep	Magnetic susceptibility, in centimeter-gram-second (CGS) units x 105 (CGS E-5)
Bulk Density	Bulk density log, in grams per cubic centimeter (g/cc)
Bedding TN	Tadpole plot of planar bedding features, oriented to True Geographic North; red body of tadpole indicates dip angle (0 to 90 degrees) along x-axis, and tail indicates the direction of dip (0 to 360-degree azimuth)
Bedding Stereo TN	Lower-hemisphere, equal-area projection of poles for planar bedding features, oriented to True Geographic North
Sonic Amplitude	Color image of the sonic amplitude log, color darkens with higher return-signal strength, in millivolts (MV)
Slowness	Log of first arrival time of sonic signal, in micro-seconds (USEC)
Caliper	Log of hole diameter measured by three-armed caliper, in inches (Inch)
Fracture Density	Number of fractures per 50-foot interval; blue indicates fracture associated with transmissive fracture zone
Fracture TN	Tadpole plot of planar fracture features oriented to True Geographic North; body of tadpole indicates dip angle, and tail indicates the direction of dip; blue indicates fracture associated with transmissive fracture zone
Fracture Stereo TN	Lower-hemisphere, equal-area projection of poles for planar fractures, oriented to True Geographic North
Blown Yield	Flow rate of blown water during air-hammer drilling, estimate indicated by black dots for flow in the 6-inch diameter hole and gray dots for flow in the 8-inch diameter hole, in gallons per minute (gal/min). Gray dots represent water measured in 8-inch hole plus the 150 gallons per minute cased off above 500 ft bls in the 6-inch hole.
Blown Spec Cond	Specific conductance of blown water during air-hammer drilling, measurement indicated by black dots for samples in the 6-inch diameter hole and gray dots for samples in the 8-inch diameter hole, in microsiemens per centimeter at 25 degrees Celsius (μS/cm @ 25°C).
Fl Res	Log of fluid resistivity collected on date indicated by color [7/23 (orange), 7/25 (blue), 8/1 (gray), 9/3 (black), and 11/14/2013 (purple) and 7/28/2014 (green)], in Ohm meters (Ohm-m)

Fl Res SD ..... Fluid resistivity of specific-depth water sample collected on date and under flow conditions as indicated by color above, in Ohm meters (Ohm-m)

Spec Cond ..... Specific-conductance log collected on date indicated by color as above, in microsiemens per centimeter at 25 degrees Celsius (µS/cm @ 25°C).

Spec Cond SD ..... Specific conductance of specific-depth water sample collected on date indicated as above, in microsiemens per centimeter at 25 degrees Celsius (µS/cm @ 25°C)

Temp ..... Temperature log collected on date indicated by color as above, in degrees Celsius (°C)

Flow Amb ..... Vertical flow rate under ambient conditions; blue circle indicates measured with electromagnetic flowmeter; blue box indicates measured with heat-pulse flowmeter; blue line indicates calculated from flow-log analysis; in gallons per minute (gal/min)

Flow Pmp ..... Vertical flow rate under pumped conditions; red dot indicates measured with electromagnetic flowmeter; red line indicates calculated from flow-log analysis; in gallons per minute (gal/min)

Trans FL ..... Transmissivity of fracture zone estimated from flow-log analysis, indicated by light blue bar, in square ft per day (ft^2/d)

Trans PI ..... Transmissivity of fracture zone estimated from packer-isolated specific-capacity data analysis, indicated by purple segment, in square ft per day (ft^2/d)

Head FL ..... Hydraulic head of fracture zone estimated from flow-log analysis (light blue dot) and packer-isolated measurement (purple segment), in ft above sea level (ft asl)

Head PI ..... Hydraulic head of fracture zone from packer-isolated measurement, indicated by purple segment, in ft above sea level (ft asl)

Spec Cond PI ..... Specific conductance of water sampled from packer-isolated interval, indicated by purple segment, in microsiemens per centimeter at 25 degrees Celsius (µS/cm @ 25 °C)

Induction Cond ..... Conductivity of the formation from induction log, in millisiemens per meter (mS/m)

Induction Res ..... Resistivity of the formation from induction log, in ohm meters (Ohm-m)

Rwa ..... Formation water resistivity estimated for selected sandstone intervals based on Archie's Equation in ohm-meters: porosity derived from log indicated in parentheses

EXPLANATION OF LITHOLOGIC SYMBOLS

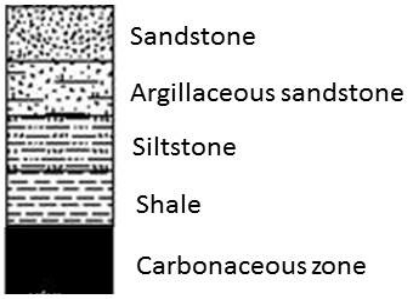

The patterns for lithologic symbols used in figures 3, 6, 10, 17, and 26 are shown to the left. Symbol colors used in the figures (not shown) are actual colors of the wet rock cuttings described in the office by staff of the Pennsylvania Bureau of Geological Survey using Munsell rock colors (Munsell, 2009).

EXPLANATION OF BEDDING AND FRACTURE TADPOLE SYMBOLS

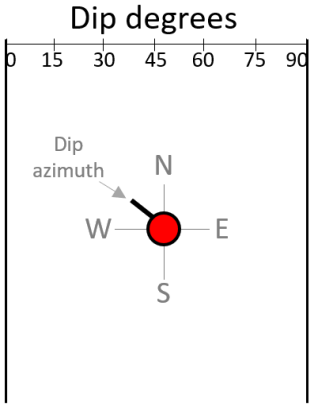

Tadpole symbols are used to designate the dip angle and direction of dip for bedding features and fractures in figures 3, 6, and 17. The position of the body of tadpole (red dot) left to right relative to the scale "Dip degrees" indicates dip angle in degrees between 0 (horizontal) and 90 (vertical). The black tail on the body of the tadpole tail indicates the direction of dip (azimuth) in degrees relative to True Geographic North. For the tadpole shown at left, the fracture dips about 45 degrees to the northwest at an azimuth of 315 degrees.

AUTHORS' NOTE

The U.S. Geological Survey and the Pennsylvania Bureau of Geological Survey use different identifiers for the test hole described in this report. Water-related borehole tests and analyses conducted in the test hole are archived by the U.S. Geological Survey as site identifier 412403076234801 and site name SU 168. Rock analyses are archived by the Bureau of Geological Survey as ID# SUL113_0297.

GEOHYDROLOGIC AND WATER-QUALITY CHARACTERIZATION OF A FRACTURED-BEDROCK TEST HOLE IN AN AREA OF MARCELLUS SHALE GAS DEVELOPMENT, SULLIVAN COUNTY, PENNSYLVANIA

by

Dennis W. Risser,[1] John H. Williams,[1] and Aaron D. Bierly[2]

ABSTRACT

The stratigraphy, water-bearing zones, and quality of groundwater were characterized in a 1,400-ft-deep test hole drilled during 2013 in fractured bedrock in Sullivan County, Pa., by collection and analysis of measurements made during drilling, geophysical logs, and depth-specific hydraulic tests and water samples. The multidisciplinary characterization of the test hole was a cooperative effort between the Pennsylvania Department of Natural Resources, Bureau of Geological Survey (BGS), and the U.S. Geological Survey (USGS). The study provided information to aid the bedrock mapping of the Laporte 7.5-minute quadrangle by BGS to help quantify the depth and character of fresh and saline groundwater in an area of shale-gas exploration (described in this report), which could help gas operators protect groundwater resources.

The Laporte test hole was drilled with air-hammer methods in an upland setting in the headwaters of Loyalsock Creek in the Glaciated High Plateau section of the Appalachian Plateaus physiographic province. Bedrock residuum and till were penetrated from land surface to 8.5 ft, the Huntley Mountain Formation of Mississippian and Devonian age was penetrated from 8.5 to 540 ft, and the Catskill Formation of Devonian age was penetrated from 540 to 1,400 ft. Fractures, determined from optical televiewer, acoustic televiewer, and video logs, were commonly encountered to 200 ft bls (below land surface), then decreased exponentially with depth, except at a highly fractured zone from 637 to 644 ft bls. Most fractures were along bedding planes and had a strike of about 243 degrees and dip about 4 degrees to the northwest, consistent with the test-hole location on the north limb of the Muncy Creek anticline. Few fractures were noted below 650 ft.

The depths of fresh and saline water-bearing fracture zones were identified in the test hole by geophysical-log analysis and were verified by pumping samples from zones isolated with packers and by collecting samples in the open hole with a wire-line point sampler. Six water-bearing zones associated with single or multiple fractures were identified at depths of 130–135, 180, 267–275, 425, 637–644, and 1,003 ft bls. Under ambient conditions, fresh water entered the hole from fractures at 130-135 and 180 ft bls, flowed downward and exited at fractures from 267–275, 425, and 637–644 ft. When pumped at 16.2 gal/min, most of the water from the open test hole was contributed from the fracture at 180 ft bls. Transmissivity, estimated from analysis of the specific-capacity data and flowmeter logs, is about

[1]U.S. Geological Survey.
[2]Pennsylvania Geological Survey.

850 ft^2/d for the entire open hole, and about 60 percent of the transmissivity is contributed from the fracture zone at 180 ft bls. The hydraulic heads in the deep water-bearing zones at 425 and 637–644 ft were about 100 ft lower than hydraulic heads in shallow water-bearing zones at 180 ft bls and above, indicating a large downward vertical hydraulic gradient.

Water samples pumped from fracture zones isolated by packers at and above the water-bearing zone at 450 ft bls were fresh with dissolved-solids contents of 105 mg/L or less. The sample isolated at 637–644 ft bls was probably affected by leakage around packers, but the specific-conductance samples collected during drilling that were believed to be representative of the fracture zone at 637–644 ft bls indicated slightly saline water. Below the 637–644 ft zone, a flowmeter log in the open hole did not detect any vertical flow, and the temperature log approached the geothermal gradient, indicating little ambient fluid flow and minimal fracture transmissivity below this depth. A petrophysical-log analysis using estimates of formation water resistivity from Archie's Equation indicated an apparent transition from fresh to saline water in the sandstones occurs between 450 to 900 ft bls, with saline water indicated below 900 ft.

Small seeps of saline water were delineated at 958, 989, and 1,003 ft bls by a time series of specific-conductance logs, and a discrete-point water sample at 990 ft bls with total dissolved-solids concentration of 19,900 mg/L verified that highly saline water was present below 900 ft bls. Occurrence of saline water at a depth of about 900 ft bls is below altitude of streams within 3 to 5 miles of the test hole but is about 930 ft above the altitude at the mouth of Loyalsock Creek where is enters the West Branch Susquehanna River at Montoursville, Pa. The depth to saline water in this test hole is close to depths estimated at two other deep test holes drilled by the BGS in upland settings in Bradford and Tioga Counties in northern Pennsylvania.

The saline water from 990 ft bls had a chemical composition similar to Appalachian Basin brines that had been diluted with fresh water. Predominant ions in the saline water were sodium, chloride, and calcium. Trace constituents of strontium, bromide, barium, lithium, and molybdenum were all more than 5,000 times greater than in freshwater samples from 167 or 270 ft bls. Methane concentration in the saline water sample from 990 ft was 120 mg/L. The concentration ratios of methane to higher-chain hydrocarbon gases and isotopic ratios of $^{13}C/^{12}C$ and $^{2}H/^{1}H$ of methane indicate that the gases are likely of thermogenic origin. In the sample from 990 ft bls, the $^{13}C/^{12}C$ of methane was less negative (-34.81 per mil) than $^{13}C/^{12}C$ of ethane (-37.1 per mil). Isotopic reversals such as this are generally found in gases from rocks older than the Catskill Formation, so its recognition in a natural upland setting at relatively shallow depth could be important when interpreting isotopic results to identify the origin of stray gas in the area.

INTRODUCTION

The Pennsylvania Department of Conservation and Natural Resources, Bureau of Geological Survey has been drilling deep exploratory test holes in several areas in northeastern Pennsylvania. Geologic information from the test holes is used to assist geologic mapping

(described in separate reports) done as part of STATEMAP, a component of the National Co-operative Geologic Mapping Program (U.S. Geological Survey, 2019a). Although the primary purpose for the drilling is to obtain detailed geologic information, the test holes also have been used to obtain hydrologic and water-quality information about the fractured-bedrock aquifers by means of cooperative studies between BGS and the U.S. Geological Survey (USGS). Results from investigations of a 1,664-ft-deep core hole in western Bradford County (Gleason test hole) and a 1,513-ft-deep core hole in south-central Tioga County (Cherry Flats test hole) have been summarized by Risser and others (2013) and Williams and others (2015), respectively.

PURPOSE AND SCOPE

This report describes investigations of a 1,400-ft-deep test hole in the Laporte 7.5-minute quadrangle in southeastern Sullivan County during 2013–14 to determine the depth and characteristics of fresh and saline groundwater in an area of shale-gas development, which could help gas operators protect groundwater resources. Drilling logs, geophysical logs, hydraulic tests, water-quality samples, and gas-isotopic data were collected and analyzed to characterize the stratigraphy and lithologies, fractures, water-bearing zones, hydraulic properties, groundwater quality, and isotopic signatures of hydrocarbons penetrated by the test hole.

DESCRIPTION OF THE LAPORTE TEST HOLE

The test hole is identified in this report as the Laporte test hole because rock cuttings and logs from the hole were used to provide stratigraphic information for the geologic mapping of the Laporte quadrangle. The Laporte test hole was located at 41.400914 degrees north latitude, 76.396756 degrees west longitude (NAD 83). The location is within Pennsylvania State Game Lands 13 in southeastern Sullivan County, about 5.2 mi east of Laporte (Figure 1). The site was selected to obtain the most complete stratigraphic section possible for rocks exposed within the quadrangle (i.e., starting in the youngest bedrock possible) and for ease of access. Land-surface altitude at the test hole site is about 2,329 ft.

The Laporte test hole was drilled to a depth of 1,400 ft bls in a broad upland setting in the headwaters of Lopez Creek, near the divide between Loyalsock Creek and Muncy Creek watersheds. The test hole was situated on the northern limb of the Muncy Creek anticline that trends NE-SW (Faill, 2011). The hole penetrated the Huntley Mountain Formation and Catskill Formation.

The bottom of the Laporte test hole at 1,400 ft bls corresponds to an altitude of 929 ft, which is below the altitudes of local and regional streams that are drains for the groundwater system. The bottom of the test hole is about 1,300 ft below the altitude of Lopez Creek, the nearest local stream and about 700 ft below Loyalsock and Muncy Creeks, the larger streams that drain the region surrounding the test hole. Although the test hole penetrates much below the surface-water drainage, it is completed about 6,000 ft above the Marcellus Formation, the development of shale gas from which has increased interest about the depth of overlying fresh groundwater resources.

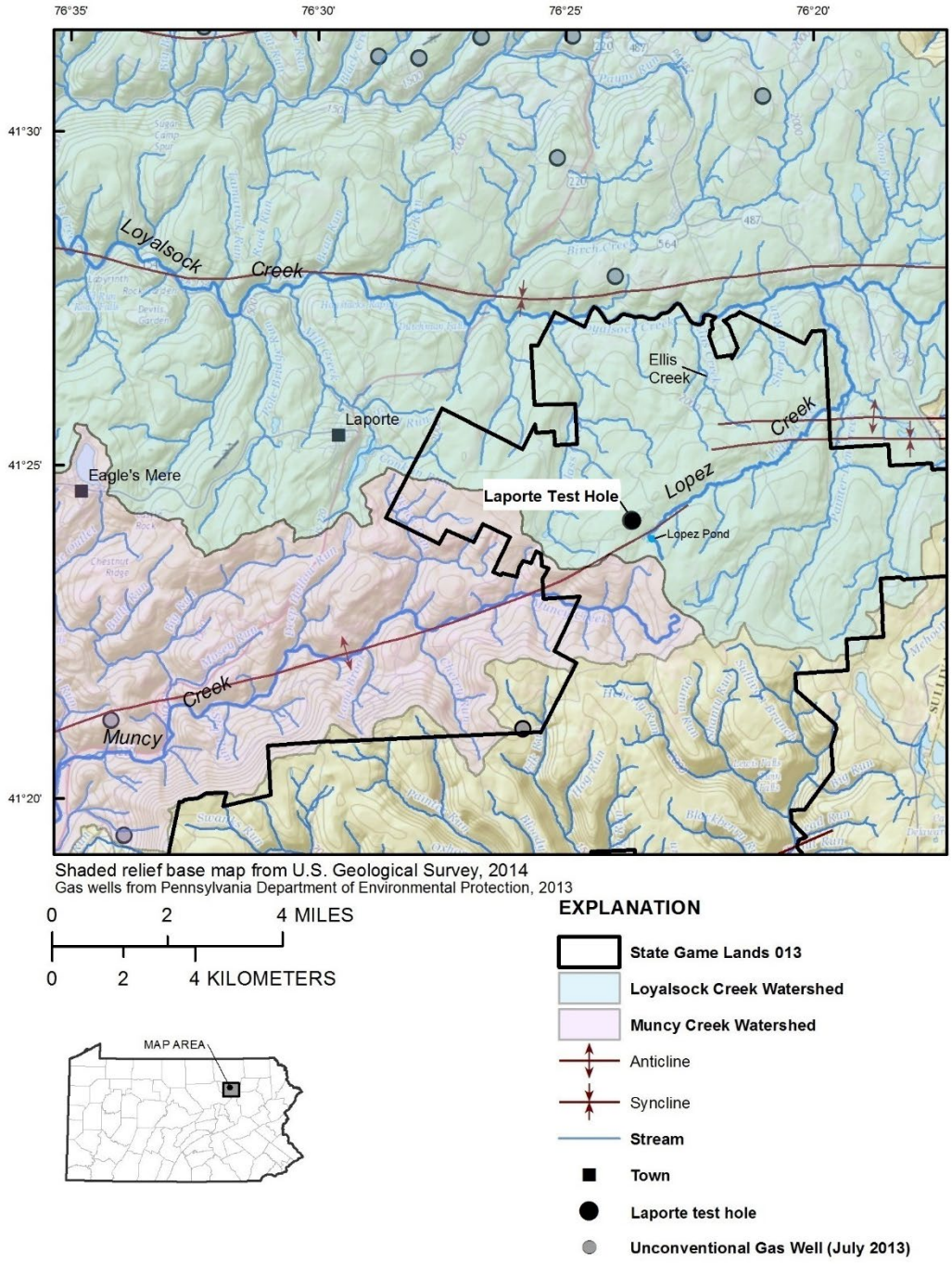

Figure 1. Location of the Laporte test hole in southeastern Sullivan County, Pa. The Muncy Creek anticline is south of the test-hole location and generally trends northeast-southwest.

METHODS

The methods used to drill the test hole and to collect and analyze the rock cuttings, geophysical logs, and depth-specific hydraulic properties and water-quality samples are described in the following sections.

DRILLING

The Laporte test hole was drilled during July 15–22, 2013, using air-hammer methods. The test hole was initiated by drilling a 10-inch hole through unconsolidated material and weathered bedrock and setting an 8.875-inch ID steel surface casing to a depth of 40 ft. bls. Beginning at 40 ft bls, an 8-inch-diameter hole was drilled to 500 ft bls. At that depth, drilling halted temporarily while the hole was cleaned by flushing with compressed air for two hours, which discharged water to the surface at a rate of about 150 gal/min. After flushing, a temporary 6.25-inch ID steel casing was set from land surface to 500 ft bls to lessen the quantity of water entering the open hole that could jeopardize the ability of the air-rotary drill rig to evacuate the water and cuttings as the hole was deepened. Drilling was completed by advancing a 6-inch-diameter hole from 500 ft bls to total depth of 1,400 ft bls. After drilling, the entire hole was developed by flushing with compressed air and foam to clean the hole and ensure that the water would be as clear as possible for subsequent imaging of the borehole. Finally, to prepare the hole for study, the 6.25-inch steel casing was removed. The final disposition of the hole was: 8.875-inch steel casing from 0 to 40 ft bls, 8-inch open hole from 40 to 500 ft bls, and 6-inch open hole from 500 to 1,400 ft bls. After investigations at the test hole were completed, it was filled with bentonite grout to a depth of 219 ft bls on September 12, 2014. On April 10, 2017, the upper 219 ft of the test hole was reconstructed with 2.5-inch-diameter PVC casing and screen for use as a monitoring well in the Pennsylvania Groundwater Quality Monitoring Network.

MEASUREMENTS DURING DRILLING

During air-hammer drilling of the Laporte test hole, compressed air forced the rock cuttings and water from the test hole to the surface, where they were routed away from the test hole into a hydrocyclone to separate cuttings from water. Cutting samples were collected at the cyclone to represent the rocks penetrated every three ft during drilling. They were briefly described, labeled, and bagged in the field. A detailed physical description of the cuttings was later prepared in the office by BGS, using standard methods and including such characteristics as lithology, Munsell color, grain size, grain shape, relative carbonate content, abundance of carbonized material, and other pertinent information. A detailed description and geologic log of rock cuttings from the test hole are available upon request from BGS.

The flow rate of water blown to the surface during drilling was estimated in a ditch downstream from the cyclone with a calibrated bucket and stopwatch when the driller blew water out of the hole before installing a new 20-ft section of drilling rod. The specific conductance and temperature of the blown water also was measured with a multiparameter water-quality meter as it discharged from the cyclone.

Water used for drilling was obtained from Ellis Creek about 3 miles north of the test hole. The water had a very low concentration of dissolved solids, as indicated by the specific conductance of the water in the creek of less than 20 μS/cm at 25°C as measured on July 16, 2013.

GEOPHYSICAL LOGS

Caliper, deviation, nuclear, electric, induction, sonic, image, and fluid logs were collected from the test hole. The nuclear logs were gamma, neutron, and gamma-gamma logs. Electric logs were self-potential, single-point resistance, and normal resistivity. The image logs were video, acoustic televiewer, and optical televiewer. The fluid logs were temperature, fluid resistivity, and flow. The geophysical logs were collected between July 23, 2013, and July 28, 2014 (Table 1). Geophysical logs collected and processed by ARM Geophysics under contract with the BGS are designated as such in Table 1.

The geophysical logs collected for this study are available for download in Log Ascii Standard (LAS) and Portable Document Format (PDF) formats from the USGS GeoLog Locator (U.S. Geological Survey, 2019b). The geophysical logs are briefly summarized below. Additional information on these types of geophysical logs is presented in Kelley (1969), Keys (1990), and Rider and Kennedy (2011).

Caliper logs record hole diameter and are collected with a probe equipped with one or three spring-loaded arms. Changes in test hole diameter may be correlated to drilling and construction procedures, competency of lithologic units, and fractures. Stationary flowmeter measurements were collected in competent intervals above and below potential fracture zones as identified on the caliper and optical and acoustic televiewer logs.

Deviation logs measure the vertical deviation and spatial trajectory of the test hole with two inclinometers and a three-component magnetometer. The deviation logs are used to correct the apparent orientation of structural features identified on the acoustic and optical televiewer logs to their true orientation.

Gamma logs measure the amount of gamma radiation emitted by the formation surrounding the test hole. Clay-bearing rocks commonly emit relatively high gamma radiation because they include weathering products of potassium feldspar and mica and tend to concentrate uranium and thorium by ion absorption and exchange. Naturally occurring sources of gamma radiation include potassium-40 and daughter products of the uranium- and thorium-decay series. The vertical resolution of the gamma tool is 1 to 2 ft. The gamma log was used in the delineation of lithology, specifically identification of sandstone, claystone, and carbonaceous zones.

Neutron logs measure the number of neutrons received at a detector from a neutron source in the probe after the neutrons have interacted with the formation surrounding the test hole. The majority of the neutron interactions are in response to the amount of hydrogen present, which is largely a function of the water content. Total formation porosity was estimated from the neutron log. Neutron logs commonly correlate with gamma logs because zones with high estimated porosities (low neutron count rates) are commonly associated with clay-bound water.

Gamma-gamma logs measure the bulk density of the formation surrounding the test hole based on the attenuation of radiation emitted from a gamma source and received at two detectors. The gamma-gamma log was converted to quantitative estimates of density.

Spontaneous-potential logs (sometimes referred to as SP or self-potential) measure the electrical potentials that develop in the test hole at lithologic and water-quality interfaces. Spontaneous potential is largely a function of chemical reactions that occur within the test hole fluids and the type and quantity of clay present. Electrochemical effects tend to result from the migration of ions from more concentrated to less concentrated fluids.

Single-point resistance logs measure the electrical resistance from points within the test hole to an electrical ground at land surface. In general, resistance increases with increasing grain size and decreases with increasing test-hole diameter, fracture density, and dissolved-solids concentration of the water. Single-point resistance logs are affected by the dissolved-solids content of the test hole fluid. The single-point resistance log was used in the delineation of lithology and fracture zones.

Normal-resistivity logs measure the electrical resistivity of the rocks and water surrounding the test hole. Electrical resistivity measurements consist of short-normal (16 inches) and long-normal (64 inches) resistivities, or near and far resistivities, respectively, that have two different volumes of investigation. Electrical resistivity measurements are affected by the clay content and porosity of the rocks and by the dissolved-solids concentration of the pore fluid. The normal-resistivity logs are most effective in formations having high electrical resistivities (low conductivities).

Magnetic-susceptibility logs measure the concentration of magnetite and other magnetic minerals present in the rocks surrounding the test hole. The magnetic susceptibility log was used in the delineation of lithology and mineralogy along with gamma, gamma-gamma, and neutron logs.

Full-waveform sonic logs measure the amplitude and transit time of acoustic waves transmitted through rocks and water surrounding the borehole. The sonic tool is equipped with a single transmitter operated at a frequency of 24 kHz and dual receivers spaced approximately 2 and 3 ft from the transmitter. Compressional wave slowness, in units of microseconds per foot (the inverse of velocity) was estimated from the acoustic travel times. Slowness is affected primarily by rock elastic properties and commonly correlates with density. Slowness also increases substantially where rocks are highly fractured.

Induction-conductivity logs measure the electrical conductivity of rocks and water surrounding the test hole. The induction tool, which is operated at a frequency of 40 kilohertz (kHz), has a focused radius of investigation and a vertical resolution of about 2 ft. The tool response generally is not affected by the electrical properties of the test hole fluid for diameters less than 8 inches. Electrical conductivity measurements are affected by the clay content and porosity of the rocks and by the dissolved-solids concentration of the pore fluid. Induction-conductivity logs are most effective in formations having high electrical conductivities (low resistivities). The induction-conductivity log was converted to an induction-resistivity log and used along with the gamma and neutron porosity logs to estimate fluid resistivity of the pore fluid in selected sandstone intervals through application of Archie's Equation (Archie, 1942).

Video logs record images of the test hole collected with a submersible color camera. Video logging techniques and equipment are described by Johnson (1996). Down-looking fisheye views of the test hole and side-looking views of the test-hole wall were recorded. The video logs were used to identify lithology, bedding and fractures, test-hole-wall staining, and water flow including cascading water above the water level, particle movement below the water level, shimmering fluid indicating saline water, and bacterial growth. For this test hole, the true depth of the video logs is estimated by multiplying the displayed depth by 1.0027 to account for stretching of the cable.

Acoustic-televiewer (ATV) logs record a 360-degree magnetically oriented acoustic image of the test-hole wall (Williams and Johnson, 2004). Acoustic-televiewer logs can be collected in clear or turbid water. The ATV provides high-resolution information on test-hole-wall roughness and the location and strike and dip of fractures or bedding within a borehole such that structural features with widths greater than 0.02 ft (6 mm) can easily be identified.

Optical-televiewer (OTV) logs record a 360-degree oriented optical image of the test-hole wall (Williams and Johnson, 2004). The OTV logs can be collected above the water level, and below water where the water is clear. Features with widths greater than 0.008 ft (2.4 mm) can be identified. OTV logs were used to characterize bedding and fracture orientation, and test-hole-wall staining.

Fluid-temperature logs measure the temperature of the air and water in the test hole. Repeated temperature logs were collected from the test hole under ambient and pumped conditions. Temperature gradients less than the geothermal gradient in the surrounding rocks indicate intervals with vertical test hole flow. As test hole flow decreases, the temperature gradient of the test hole water approaches the geothermal gradient. Downflow is characterized by test hole water cooler than that in equilibrium with the geothermal gradient. Conversely, upflow is characterized by test hole water warmer than that in equilibrium with the geothermal gradient. The geothermal gradient is about 1°F (0.56°C) per 100 ft (Keys, 1990). Temperature logs were used with the fluid-resistivity, specific conductance, and flow logs to identify fracture zones and flow between them under ambient and pumped conditions.

Fluid-resistivity logs measure the electrical resistivity of the water in the test hole. The electrical resistivity of the water is related to its dissolved-solids concentration. Repeated fluid-resistivity logs were collected under ambient and pumped conditions. Specific-conductance logs were calculated from the fluid resistivity and the temperature logs. Fluid-resistivity and specific-conductance logs were used with the temperature and flow logs to identify freshwater and saline-water fracture zones and flow between them under ambient and pumped conditions.

Flow logs record the direction and rate of vertical flow in the test hole. Flow logs were collected from the test hole under ambient conditions and while pumping at a constant rate with quasi-steady-state drawdown. Heat-pulse and electromagnetic flowmeters were used to measure vertical flow. The heat-pulse flow meter measures the travel time of a thermal pulse between a set of upper or lower thermistors (Hess, 1982). The heat-pulse flowmeter, which was used in a stationary mode with a flexible rubber diverter fitted to the nominal

diameter of the test hole, has a measurement range of 0.01 to 1.5 gal/min. The electromagnetic flowmeter (Young and Pearson, 1995) measures fluid velocity based on Faraday's Law, which states that the flow of an electrically conductive fluid through an induced magnetic field generates a voltage gradient that is proportional to its velocity. The electromagnetic flowmeter, which was used in stationary and trolling modes with a flexible rubber diverter, has a measurement range of 0.05 to 15 gal/min. The flow logs were used with the temperature and fluid-resistivity logs to identify fracture zones and the direction and rate of flow between zones under ambient and pumped conditions.

Table 1. *Types of Geophysical Logs and Dates of Collection from the Laporte test hole, Sullivan County, Pa.*

(Agency: ARM, ARM Geophysics; USGS, U.S. Geological Survey; X, log collected; --, not collected.)

Logs collected	Agency or company collecting the geophysical logs and date(s) collected							
	ARM	USGS	USGS	USGS	USGS	USGS	USGS	USGS
	8/1-2/2013	7/23-25/2013	7/30/2013	8/5/2013	9/3/2013	11/7/2013	11/14/2013	7/28/2014
Three-arm caliper	X	X	--	--	--	--	--	--
Deviation	X	X	--	--	--	--	--	--
Natural gamma	X	X	--	--	--	--	--	--
Neutron	X	--	--	--	--	--	--	--
Gamma-gamma	X	--	--	--	--	--	--	--
Spontaneous potential	X	--	--	--	--	--	--	--
Single-point resistance	X	--	--	--	--	--	--	--
Normal resistivity	X	--	--	--	--	--	--	--
Magnetic susceptibility	--	X	--	--	--	--	--	--
Full waveform sonic	--	X	--	--	--	--	--	--
Induction conductivity	--	X	--	--	--	--	--	--
Video	--	--	X	--	--	X	--	--
Acoustic televiewer	--	X	--	--	--	--	--	--
Optical televiewer	X	X	--	--	--	--	--	--
Fluid temperature	X	X	--	X	X	--	X	X
Fluid resistivity	X	X	--	X	X	--	X	X
Flow	--	X	--	--	--	--	--	--

The ambient and pumped flow logs were analyzed using the method described by Paillet and others (1987) and Paillet (2000) to estimate the transmissivity and hydraulic head of the fracture zones penetrated by the test hole. In this method, a best-fit match is developed

between measured and model-calculated ambient and pumped flows by iterative adjustment of flow-zone transmissivity and hydraulic head in a numerical or analytical model. The flow-log analysis method generally detects and quantifies the hydraulic properties of fracture zones whose transmissivities are within 1.5 to 2 orders of magnitude of the most transmissive zone penetrated by the borehole (Paillet, 1998). The computer model FLASH (Flow Log Analysis of Single Holes) developed by Day-Lewis and others (2011) was used to solve for flow-zone transmissivity and head. The FLASH model code is based on the Thiem equation, which is a multilayer, analytical solution for steady-state radial flow to a single borehole. The solution requires that the total borehole transmissivity or the radius of influence is independently estimated. The total transmissivity of the open test hole was estimated from the specific capacity of the open hole.

AQUIFER ISOLATION WITH PACKERS

The principal water-yielding fractures in the test hole identified during drilling and by analysis of the geophysical logs were temporarily isolated for water sampling and hydraulic testing by use of a straddle-packer-and-pump system during August 6–29, 2014. The main purpose for isolating the fractures was to enable the collection of water samples from different depth zones, but the packer system also allowed hydraulic tests to be conducted. Five depth intervals were isolated by the packers (Table 2). Prior to installing packers, the condition of the slightly rugose test-hole wall created by the air-hammer was examined with the video camera to verify that the borehole where the packer would sit was relatively smooth and unfractured to improve the odds of achieving a good packer seal.

Table 2. *Depth of the intervals temporarily isolated by the use of packers, major water-bearing fractures isolated, and sample-pump setting in the Laporte test hole, Sullivan County, Pa.*

Zone	Single or straddle packer used to isolate the interval	Geologic Formation	Depth, in ft below land surface		
			Intervals isolated by packers	Major water-bearing fracture zone	Depth of sample pump
1	single	Huntley Mountain	Above 172	130-135	167
2	straddle	Huntley Mountain	172 to 197	180	180
3	straddle	Huntley Mountain	263 to 288	267-275	270
4	straddle	Huntley Mountain	418 to 443	425	437
5	straddle	Catskill	621 to 646	637-644	640

Two packers were assembled on a 1.25-inch ID steel pipe and spaced to allow a 25-ft interval of the test hole to be temporarily isolated (straddled). A 4-inch submersible pump was installed on the steel pipe between the packers. The pump removed water from the isolated interval and discharged it to land surface in a 0.75-inch ID polyethylene tubing attached to outside of the 1.25-inch steel pipe. The packers were inflated with nitrogen from a cylinder of the compressed gas. Hydraulic head was monitored above, within, and below the straddled zone using barometrically compensated pressure transducers deployed within

1-inch PVC pipes that were connected to nylon tubes open above, within, and below the straddled zone (Figure 2).

The general procedure for isolating a zone was to position the packers straddling a water-yielding fracture, inflate the upper packer and then inflate the lower packer while continuously monitoring the hydraulic heads above, within, and below the isolated interval until a quasi-steady-state equilibrium was reached. The length of time that the packers were left inflated before the interval was tested ranged from 0.78 to 137 hours, depending on how quickly the hydraulic head equilibrated after packer inflation. The isolated intervals were then pumped at rates ranging from 1.3 to 10.6 gal/min so water samples could be collected. Drawdown of water levels was recorded above, within, and below the isolated interval during the pumping.

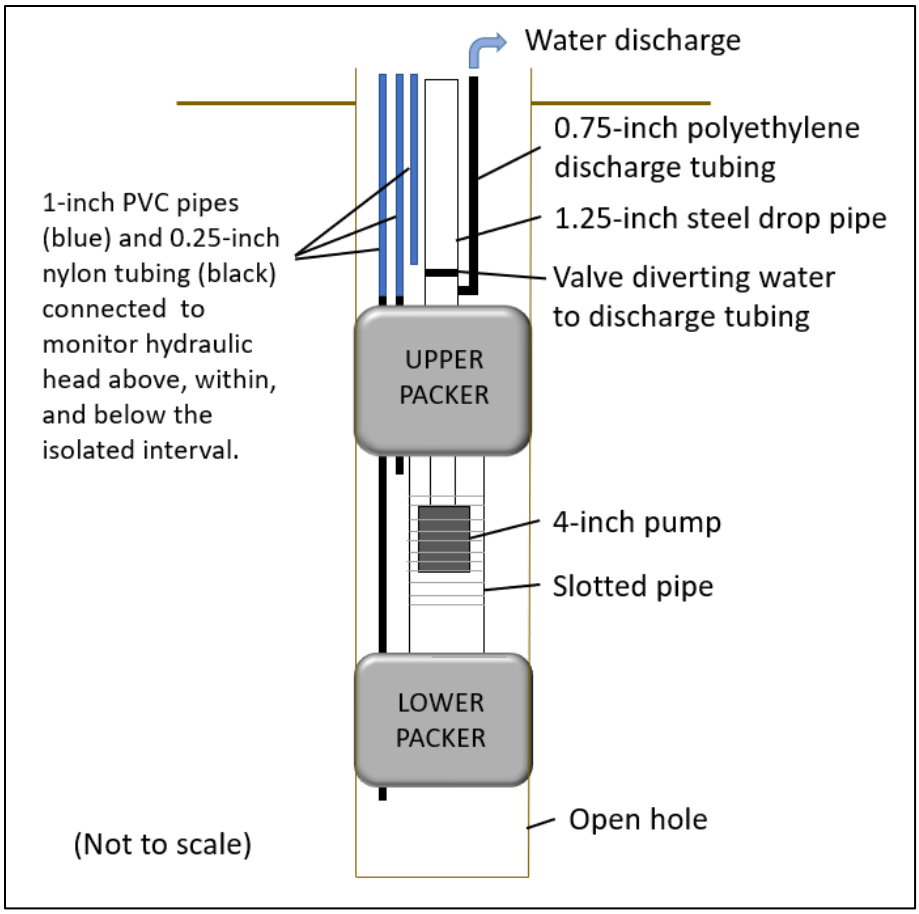

Figure 2. Schematic diagram of packer assembly used to isolate water-yielding fractures in the Laporte test hole.

HYDRAULIC TESTS

Drawdown data were collected during pumping of the open hole and intervals isolated with packers. Specific capacity and transmissivity were determined from analysis of the drawdown data.

Open-Hole Hydraulic Test

The open test hole was pumped at a constant rate of 16.2 gal/min for 60 minutes on July 25, 2013, and water-level drawdown was recorded with a pressure transducer. The specific capacity of the open hole was determined by dividing the pumping rate (Q) by the quasi-steady-state drawdown (s) after one of hour of pumping. The transmissivity of the open test hole was estimated from the specific capacity (Q/s) of the test hole from an equation from Cooper and Jacob (1946) as described in Theis and others (1963). But instead of using the nomograph in the Theis and others paper, the Cooper-Jacob equation (Eq. 1) was solved for transmissivity (T) using an iterative approach after assigning a reasonable value for storage coefficient (S).

$$T = \frac{Q}{4\pi s}\ ln\left[\frac{2.25Tt}{r^2S}\right] \qquad \text{Eq. 1}$$

Where:
T is transmissivity in ft squared per day,
Q is pumping rate in cubic ft per day,
s is drawdown in ft,
t is the time in days at which specific capacity is determined,
S is storage coefficient, dimensionless.

Transmissivity of the open hole also was estimated from the transient, late-time drawdown data during pumping by use of the straight-line method of Cooper and Jacob (1946). The solution for transmissivity is:

$$T = \frac{35.3\ Q}{\Delta s} \qquad \text{Eq. 2}$$

Where:
T is transmissivity in ft squared per day,
Q is pumping rate in gallons per minute,
Δs is the drawdown per log cycle of time, in ft.

Isolated-Interval Hydraulic Tests

The specific capacity of each isolated interval was determined by dividing the average discharge rate by the drawdown after about one of hour of pumping. The transmissivity of the isolated interval was estimated from specific capacity by iterative solution of the Cooper and Jacob (1946) equation as described above.

WATER-QUALITY SAMPLES

Samples were collected from five depth zones that had been isolated with packers (Table 2) and at one discrete depth from within the open hole. Field and laboratory analysis of water samples provided information about the quality of water in the test hole at specific depths.

Samples were collected for analysis of field parameters, major ions, trace metals, radiochemicals, dissolved gases, and isotopic composition. The pH, water temperature, specific

conductance, dissolved oxygen, oxidation-reduction potential, and turbidity were measured in the field with a multiparameter meter. Alkalinity was determined by titration to an inflection-point determined from titration in the field. Samples for analysis of major ions and trace metals were sent to the USGS National Water Quality Laboratory (NWQL) in Denver, Colorado. Samples for radiochemical analysis were sent to Eberline Services Inc., a private laboratory under contract to the USGS NWQL. Samples for analysis of dissolved gases and stable isotopes (except strontium) were sent to Isotech Laboratories, Inc. Strontium isotopes were analyzed by the USGS Crustal Geophysics and Geochemistry Science Center. The analytical results are available from the USGS

National Water Information System database at https://nwis.waterdata.usgs.gov/usa/nwis/qwdata/?site_no=412403076234801.

Isolated-Interval Samples

Isolated-interval samples were collected from the test hole during August 7–29, 2013. Water samples were obtained from 25-ft depth intervals that were temporarily isolated with packers by a 4-inch-diameter submersible pump located between the upper and lower packers. The pump discharged water through a 0.75-inch polyethylene pipe. At the surface, the discharge was split by use of a PVC valve so that a small quantity could be diverted to a multiparameter water-quality meter or to sample bottles. Prior to sampling, water from the isolated interval was purged. The rate of discharge (pumping rate) was determined during the purging period by volumetric method using a bucket and stopwatch. The discharge from the isolated interval was monitored until three volumes of water were removed from the isolated interval and stability of the field water-quality parameters (specific conductance, temperature, pH, and dissolved oxygen) was reached within about +/- 5 percent. Sample bottles were filled within a covered chamber, processed according to protocols outlined in Wilde and others (2002–2009), preserved with acid and chilled (as required), and shipped to the laboratory by overnight express.

Discrete-Point Samples

Two discrete-point samples were collected from the Laporte test hole at a depth of 990 ft bls. The first point-sample at 990 ft bls was collected on September 5, 2013, after the isolated-interval samples had been completed and the packers had been removed. The second sample was collected nearly one year later on July 28, 2014, to determine if the salinity at that depth had increased. The samples were collected under ambient (non-pumping) conditions by the use of a stainless-steel point sampler. The sample depth of 990 ft bls was determined by analysis of the geophysical logs, flowmeter, temperature, fluid-resistivity, and specific-conductance logs to be representative of saline water in the test hole at 900 ft bls and below. The sample at 990 ft bls would capture hydrocarbon gases rising from the main inflow at 1,003 ft bls. The point sampler was used because the depth exceeded our capacity for packer use.

The point sampler used in this study was lowered to the sampling depth where the inlet valve was remotely controlled through the wireline, which opened and closed the intake port

of the sampler, allowing as much as two liters of water to be collected. The valve was opened for about 5 minutes while the sampler filled with water; then the valve was closed, and the sampler was raised to the surface. About four liters of water was needed for laboratory analysis of the selected analytes.

After retrieving the point sampler at the surface, water was transferred into the appropriate sampling containers, processed according to protocols outlined in Wilde and others (2002–2009), preserved with acid and chilled (as required), and shipped to the laboratory by overnight express. Transfer of unfiltered samples was accomplished by opening the discharge port and allowing water to drain from the sampler into bottles. For samples requiring filtration, a 6-inch length of Teflon-lined tubing and a capsule filter with 0.45-micron-size pores was attached to the discharge port of the point sampler. A cylinder of ultra-pure nitrogen gas was attached to the intake port of the point sampler, and nitrogen gas was used to push sample water through the capsule filter, which eliminated the need to open the sampler to the atmosphere. Samples for gases and stable isotopes were collected by draining water from the point sampler or pushing it with nitrogen gas directly into a gas-sample "Isobag" without opening the sample intake port to the atmosphere.

Field properties were measured as soon as possible after water was transferred out of the point sampler and into the sample cup of the multiparameter meter, but the water samples had warmed; degassing was noted; and the values for temperature, dissolved oxygen, and oxidation-reduction potential were drifting. Thus, these field values for the point samples are not completely representative of the water at depth for those parameters.

One field blank was collected to evaluate contamination from field equipment and sampling procedures. The field blank was prepared by pouring reagent-grade inorganic-free water into the stainless-steel point sampler, then transferring the water into the appropriate sample containers in the same procedure described above for the specific-depth environmental samples.

GEOHYDROLOGIC CHARACTERIZATION

The geohydrology of the Laporte test hole was characterized through an analysis of drill cuttings, geophysical logs, and aquifer-isolation tests. The bedrock stratigraphy and lithology, fractures, and water-bearing intervals penetrated by the test hole are discussed in the following sections.

STRATIGRAPHY AND LITHOLOGY

The stratigraphy of the Laporte test hole was characterized mainly by analysis of the drill cuttings, with supporting information from natural-gamma, caliper, optical imagery, and other geophysical logs. In descending order (youngest to oldest), the test hole penetrated siliciclastic sedimentary rocks of the Lower Mississippian and Upper Devonian Huntley Mountain Formation and Upper Devonian Catskill Formation (Figure 3). Cuttings were archived at the Bureau of Geological Survey's Middletown office. They are available for public review and scientific research upon request.

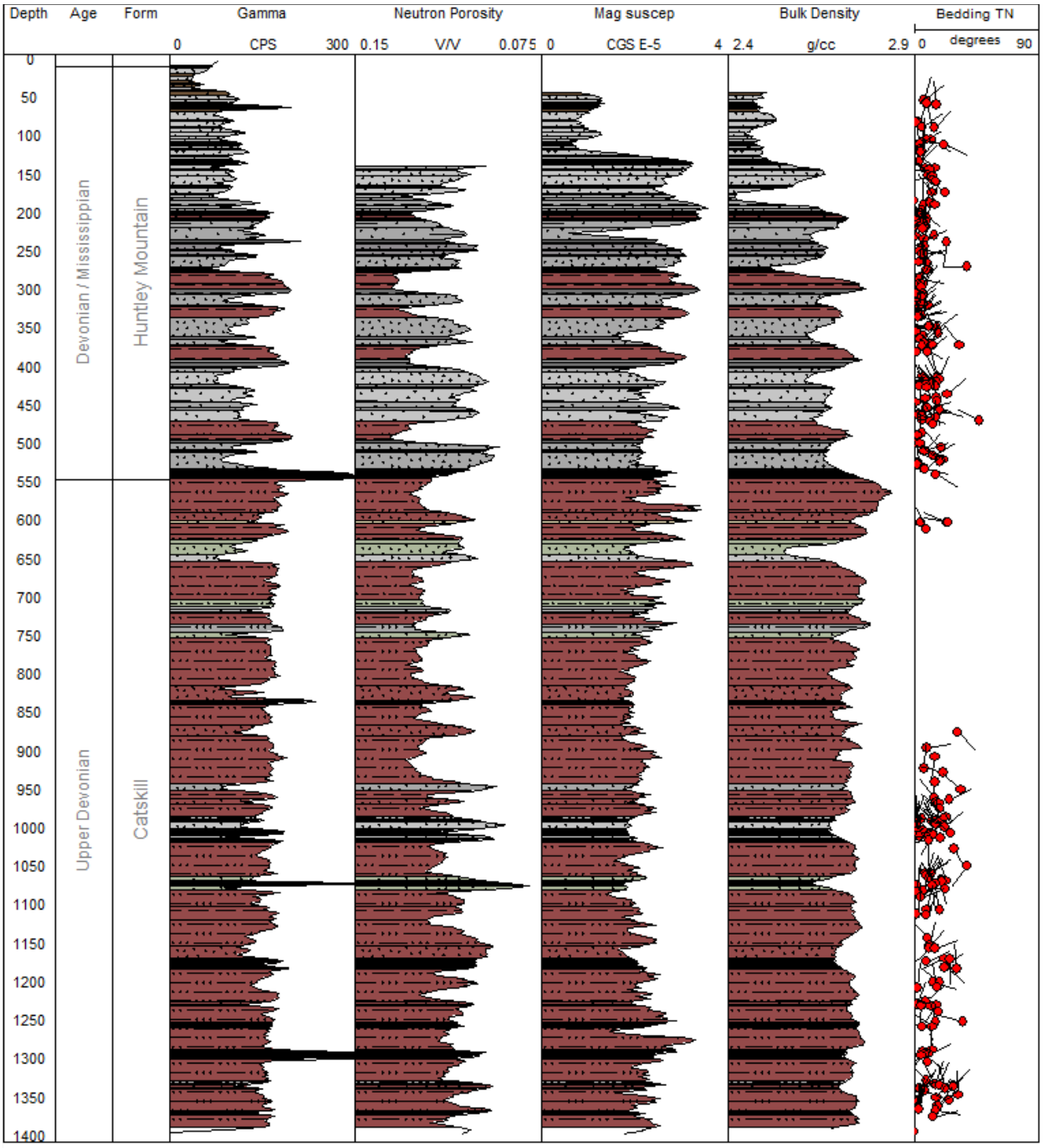

Figure 3. Logs of stratigraphy, lithology, gamma, neutron porosity, magnetic susceptibility, bulk density, and bedding orientation in the Laporte test hole, Sullivan County, Pa. (Explanation of log headings, units, symbols, and colors are presented on pages x–xii.)

Huntley Mountain Formation

The Huntley Mountain Formation was penetrated from about 8.5 to 540 ft bls. The overlying surface to 8.5 ft consisted of unconsolidated sediment (till and bedrock residuum). The Huntley Mountain Formation is a transitional unit between the underlying Catskill Forma-

tion and the overlying Burgoon Formation. The Huntley Mountain Formation consists of sandstone, siltstone, and claystone. In fresh rock, sandstones range in color (Munsell, 2009) from medium dark gray (N4) to very light gray (N8). Minor quantities of brownish-gray (5YR 6/1) sandstone were observed in relation with red-bed intervals. In weathered rocks (dominantly in the upper 20 ft), colors ranged from very pale orange (10YR 8/2) to dark yellowish brown (10YR 4/2) and yellowish gray (5Y 7/2). Sandstones range from very fine to coarse grained with most being fine to medium grained. A low density of scattered detrital mica flakes is common. Sandstones are locally slightly calcareous. A calcareous zone was observed from approximately 310 to 315 ft bls. Rare carbonaceous debris is present, and very thin coaly lenses were observed at approximately 180 ft bls and 409 ft bls (Figure 4). Pyrite was observed in association with the coaly lenses.

Thin, medium-dark-gray (N4) to medium-gray (N5) shales were observed throughout the Huntley Mountain Formation. Five red-bed intervals composed chiefly of grayish-red (5R 4/2) claystone and siltstone with subordinate amounts of light-olive-gray (5Y 6/1), bluish-gray (5B 6/1) and greenish-gray (5G 6/1) claystone and siltstone were noted. A few fossilized rootlets were observed. Red-bed intervals can be interbedded with other lithologies mentioned above and range from 15 to 29 ft thick.

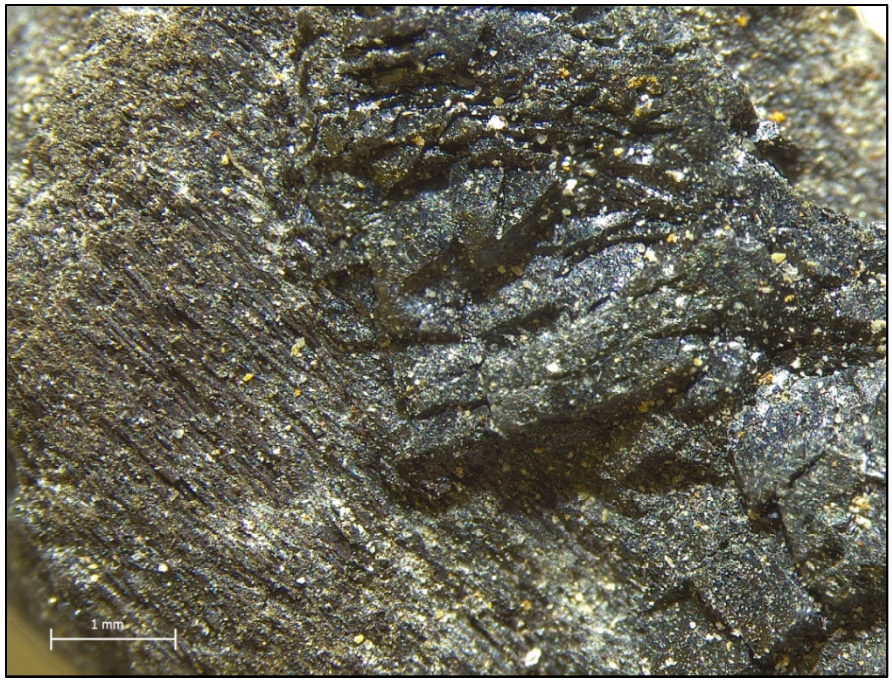

Figure 4. Test-hole cutting with fossilized plant stem impression (left half) and coal material (right half). Note the near 90° cleats in the coal. Cutting was sampled from between 178 and 181 ft bls. Note: mm = millimeter.

Catskill Formation

The Catskill Formation occurs from about 540 ft bls to the total depth of the hole at 1,400 ft bls. The Catskill Formation is distinguishable from the Huntley Mountain Formation by more abundant and thicker red-bed packages. The Catskill Formation has proportionally thinner and fewer gray sandstones than the overlying Huntley Mountain Formation.

Red beds within the Catskill are composed chiefly of grayish-red (5R 4/2) siltstone and claystone as well as brownish-gray (5YR 4/1 to 5YR 6/1) sandstone. The brownish-gray

sandstones are mostly very fine to medium grained, slightly micaceous to micaceous, and locally calcareous. Subordinate amounts of medium-gray (N5) to very light gray (N8) sandstone like those in the Huntley Mountain Formation were observed. Within one of these gray sandstone intervals, cuttings of very pale orange (10YR 8/2), coarsely crystalline calcite vein with clear quartz crystals were observed at approximately 638 to 642 ft bls (Figure 5).

Figure 5. Test-hole cutting from a calcite vein (right half) with clear quartz crystals (upper left corner). Cutting was sampled from between 640 to 642 ft bls.

FRACTURES, BEDDING, AND BREAKOUTS

The distribution and orientation of fractures, bedding features, and breakouts, from the bottom of the casing at 40 ft bls to the total depth of the hole at 1,400 ft bls, were determined through the analysis of the optical televiewer log, modified by information from the acoustic televiewer and video logs. Fracture density (number of fractures divided by the depth interval length) for 50-ft intervals is shown by the bar graph in Figure 6. Fracture density increased with depth from the base of casing to 100 ft bls, then generally decreased with depth to the bottom of the hole except for a notable increase at the highly fractured zone from 637 to 642 ft bls. The interval from 50 to 200 ft bls was most fractured; about 21 fractures were penetrated every 50 ft in that interval. Below 642 ft bls there is a marked decrease in fracture density to about 1.6 per 50 ft of hole. A plot of the cumulative frequency of fractures with depth shows that fractures decrease exponentially with depth (Figure 7). About 80 percent of the fractures penetrated by the test hole were low-angle features dipping less than 20 degrees in all directions (Figure 8). About 6 percent of the fractures had steep dips (greater than 45 degrees) to both the northwest and southeast.

Bedding features penetrated by the test hole were planar with noticeable crossbedding. The mean strike of bedding planes was about 243 degrees (N67E) with a mean dip of about 4 degrees northwest (Figures 3 and 8B). Although displaying scatter due to the low bedding

angle and abundant crossbedding, the mean bedding orientation was consistent with the position of the test hole on the northern limb of the Muncy Creek anticline (Figure 1).

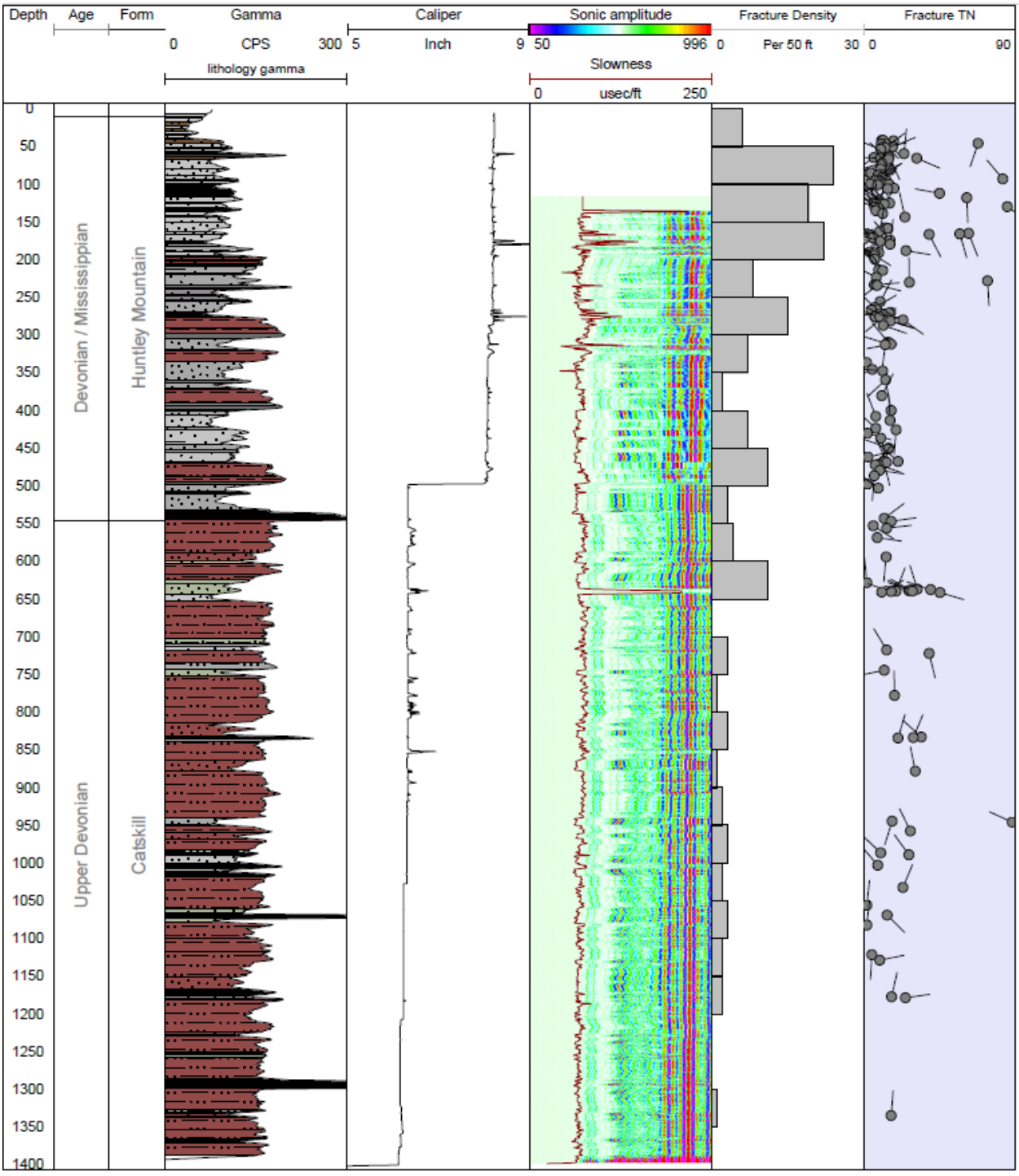

Figure 6. Logs of stratigraphy, lithology, gamma, caliper, sonic amplitude and slowness, and fracture density and orientation in the Laporte test hole, Sullivan County, Pa. (Explanation of log headings, units, colors, and symbols are presented on pages x–xii.)

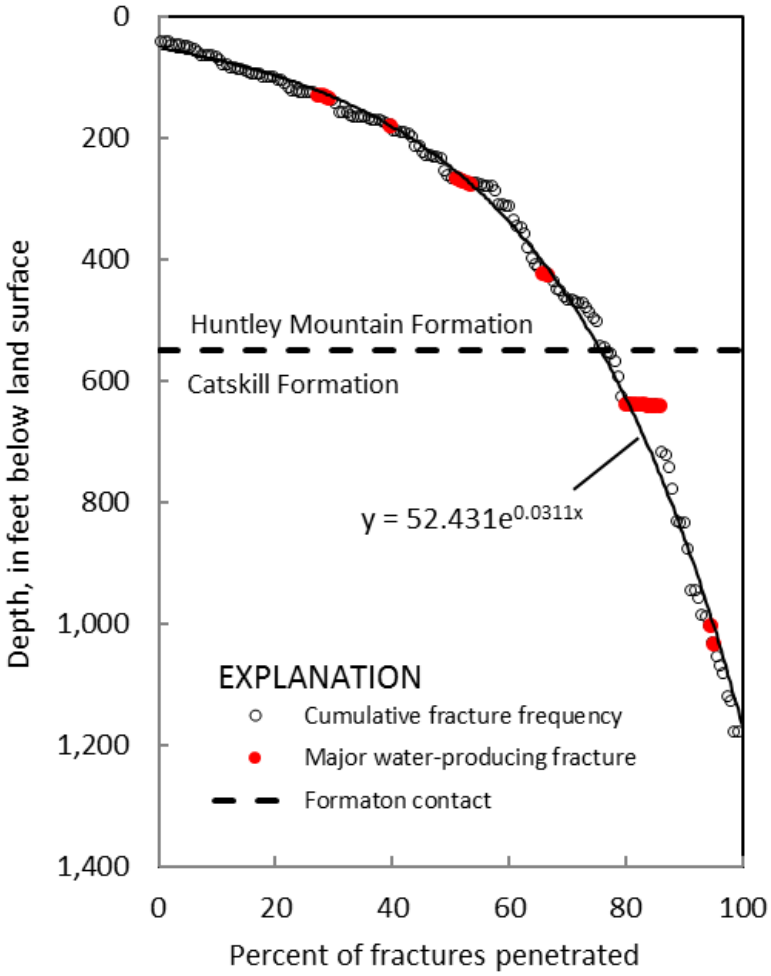

Figure 7. Cumulative frequency of penetrated fractures in relation to depth below land surface in the Laporte test hole, Sullivan County, Pa.

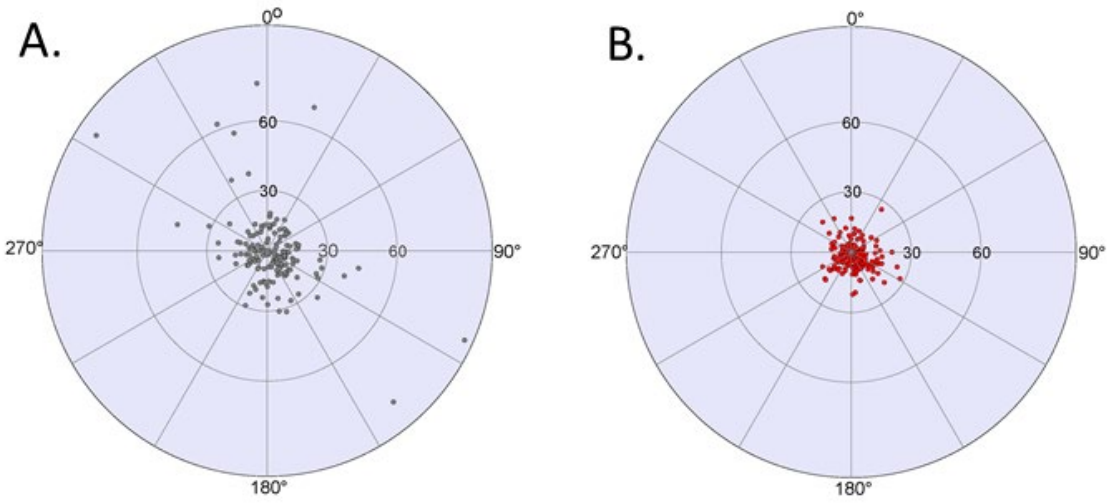

Figure 8. Lower-hemisphere, equal-area projection of poles to planes of (A) fractures and (B) bedding planes penetrated by the Laporte test hole, Sullivan County, Pa.

Breakouts are formed by spalling of bedrock fragments from the open test-hole wall parallel to the modern-day direction of minimum horizontal stress exerted on the rocks. Breakouts were clearly identified at various depths within the Catskill Formation. For example, the vertically aligned pairs of borehole-enlargement features discontinuously present on the ATV log from 756 to 808 and 880 to 938 ft bls presumably are breakouts (Figure 9). These features were oriented similarly to breakouts more clearly identified in the test holes in Bradford and Tioga Counties (Risser and others, 2013; Williams and others, 2015), in which the water was much less turbid, allowing better imaging of the test-hole walls. The breakout orientation in the Laporte test hole indicated that the direction of maximum modern-day horizontal stress on the rocks is at an azimuth of about 70 degrees (northeast to southwest), which is consistent with regional estimates presented by Zoback and Zoback (1980).

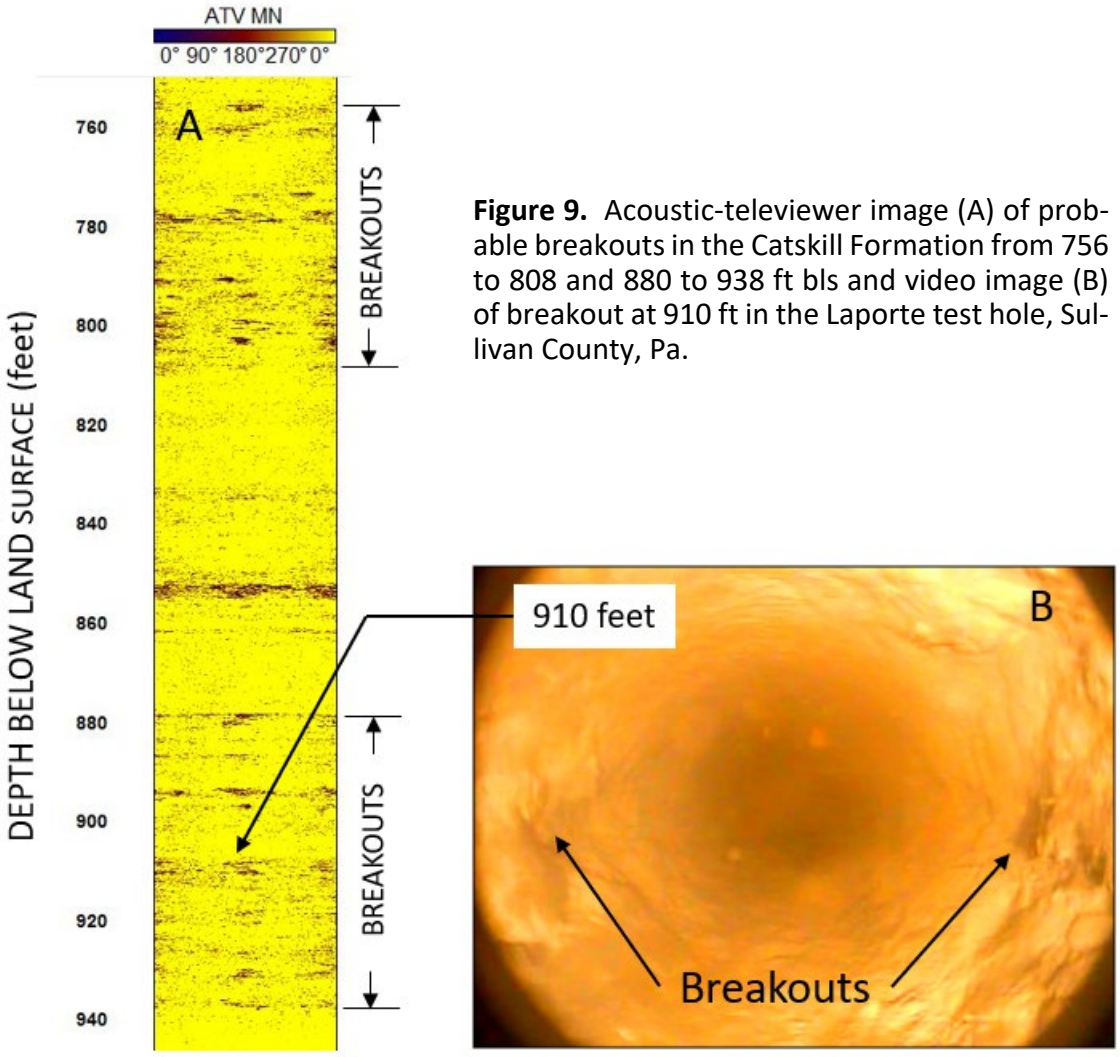

Figure 9. Acoustic-televiewer image (A) of probable breakouts in the Catskill Formation from 756 to 808 and 880 to 938 ft bls and video image (B) of breakout at 910 ft in the Laporte test hole, Sullivan County, Pa.

WATER-BEARING FRACTURES

The transmissive water-bearing fractures penetrated by the test hole were identified through measurements of water discharge from the hole during drilling and through analysis of the fluid-temperature, fluid-resistivity, specific-conductance, fluid-flow, and video logs, in conjunction with the fracture descriptions presented in the previous sections (Figure 10). Six water-bearing zones associated with single or multiple fractures were identified at depths of 130–135, 180, 267–275, 425, 637–644, and 1,003 ft bls.

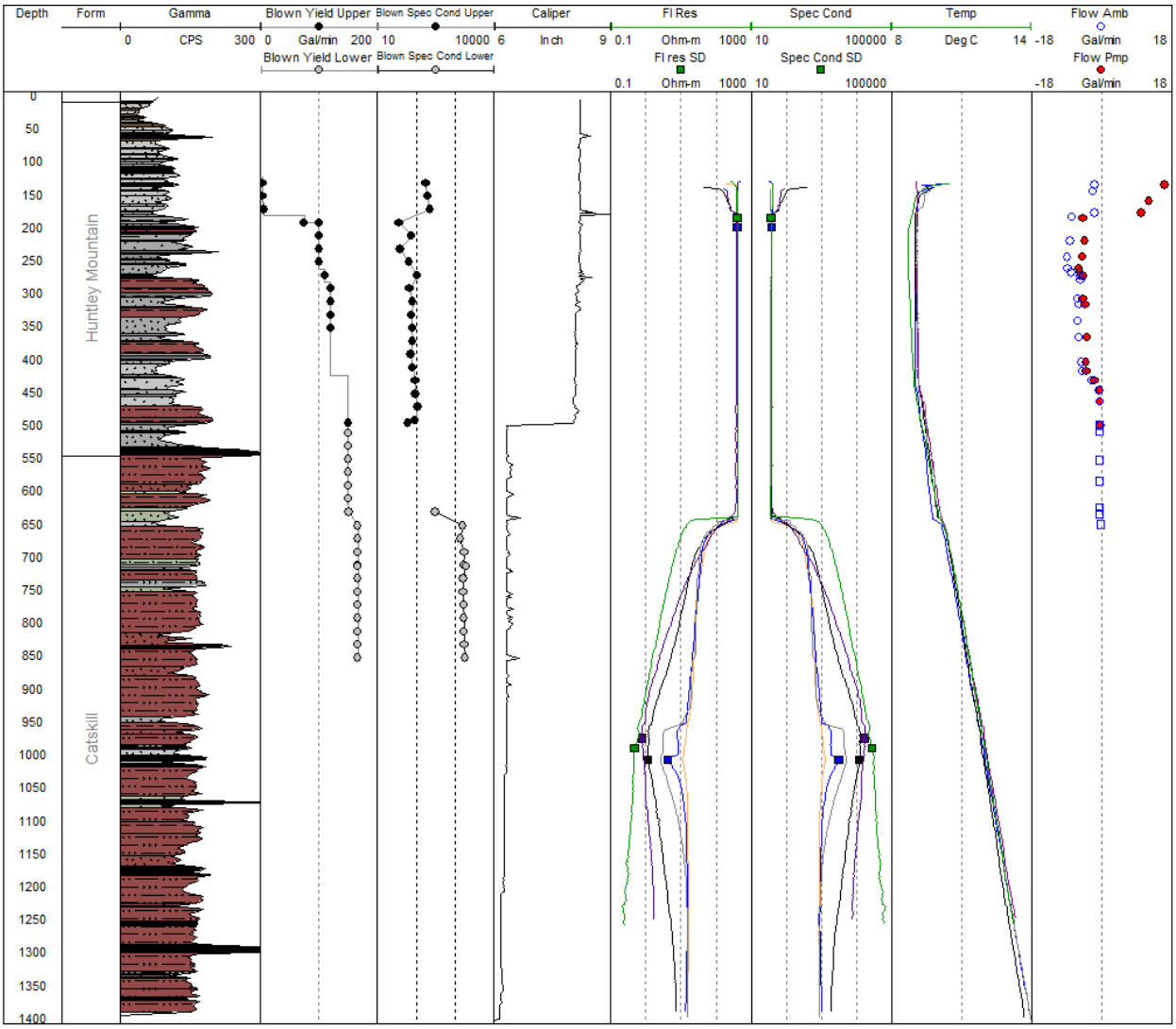

Figure 10. Logs of stratigraphy, lithology, gamma, caliper, fluid resisitivty, temperature, specifc conductance, flow, and fracture orientation in the Laporte test hole, Sullivan County, Pa. (Explanation of log headings, units, symbols, and colors are presented on pages x–xii.)

Fracture Zone 1—130 to 135 ft

The freshwater-bearing zone at 130–135 ft bls was associated with several bedding-related fractures and a steeply dipping fracture in interbedded sandstone and carbonaceous shale (Figure 11). The air-blown yield from the zone was about 5 gal/min during drilling. After completion of the test hole, the fluid-flow logs showed that about 1 gal/min of water entered from the zone and flowed down under ambient (non-pumping) conditions. Some of the downflow was cascading, which could be seen on the video log. When the open test hole was being pumped at 16.2 gal/min, about 4 gal/min entered from the zone. The water level in the open hole during the study fluctuated across this fracture zone, which probably caused the yield from the zone to vary.

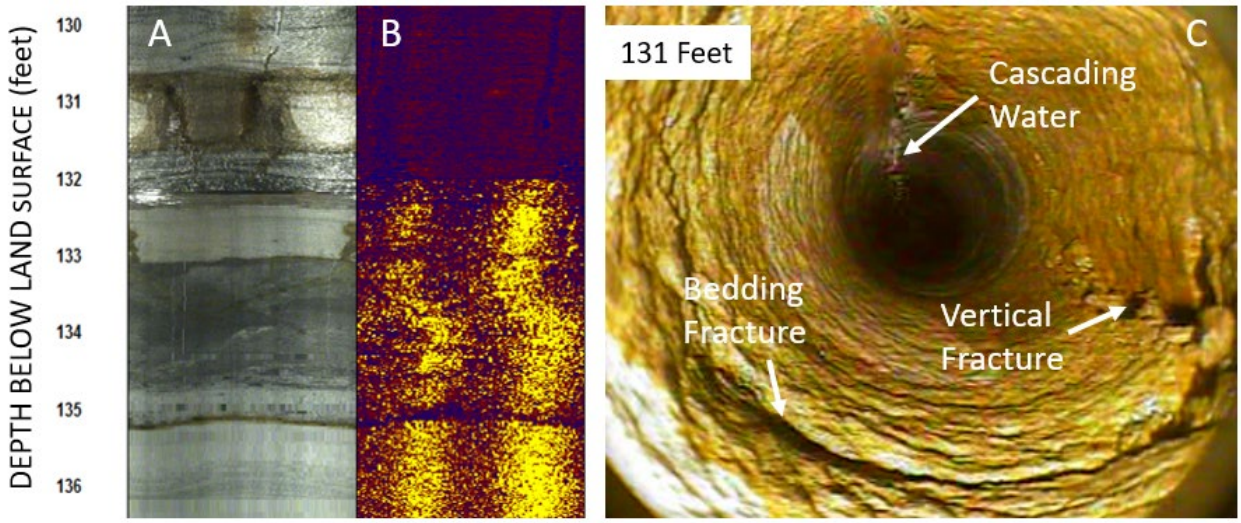

Figure 11. Water-bearing zone at 130–135 ft bls associated with steeply dipping and bedding-related fractures in interbedded sandstone and carbonaceous shale: A) optical-televiewer image, B) acoustic-televiewer image, and C) video image.

Fracture Zone 2—180 ft

A major freshwater-bearing zone was identified at 180 ft bls where the test hole penetrated a large, subhorizontal fracture in sandstone as shown by an enlargement of the hole on the caliper log (Figure 10) and on image and video logs (Figure 12). The air-blown yield from this fractured zone was about 100 gal/min during drilling, by far the greatest yield of all the penetrated zones. After completion of the test hole, the fluid-flow logs showed that the zone yielded more than 7 gal/min of downflow under ambient open-hole conditions, and more than 12 gal/min of upflow along with about 6 gal/min of downflow when the open test hole was pumped at 16.2 gal/min.

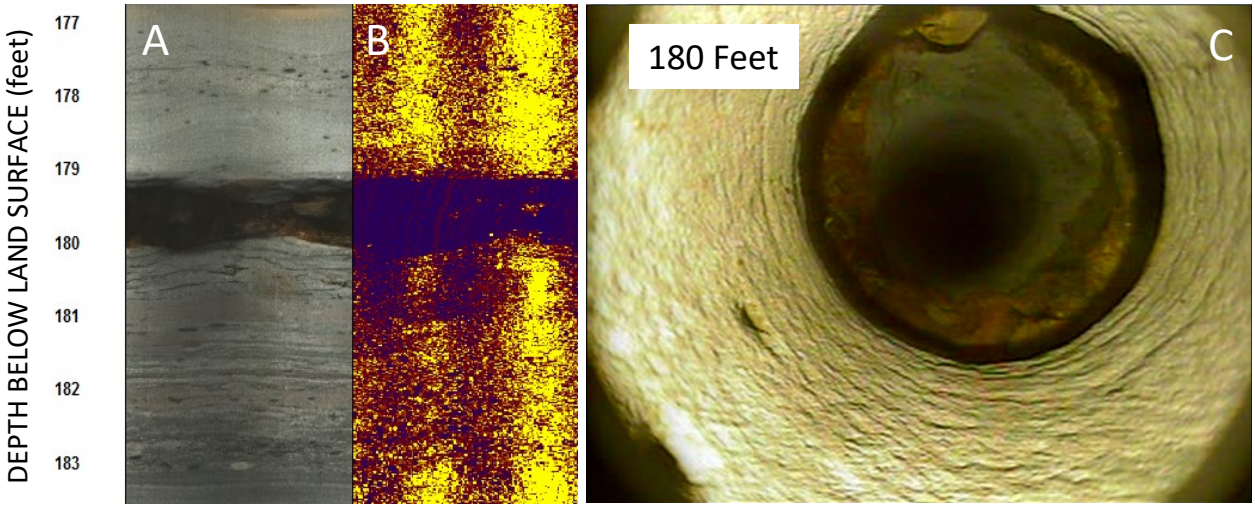

Figure 12. Water-bearing zone at 180 ft bls associated with subhorizontal fractured zone in sandstone: A) optical-televiewer image, B) acoustic-televiewer image and C) video image.

Fracture Zone 3—267 to 275 ft

The water-bearing zone at 267–275 ft bls was associated with multiple bedding-related fractures in sandstone above a contact with red shale as shown by an enlargement of the hole on the caliper log (Figure 10) and on image and video logs (Figure 13). The air-blown yield attributed to this zone during drilling was about 20 gal/min. After completion of the test hole, the fluid-flow logs showed that about 3 gal/min of the downflow exited the zone under ambient open-hole conditions, which was reduced to less than 1 gal/min when the open test hole was pumped at 16.2 gal/min.

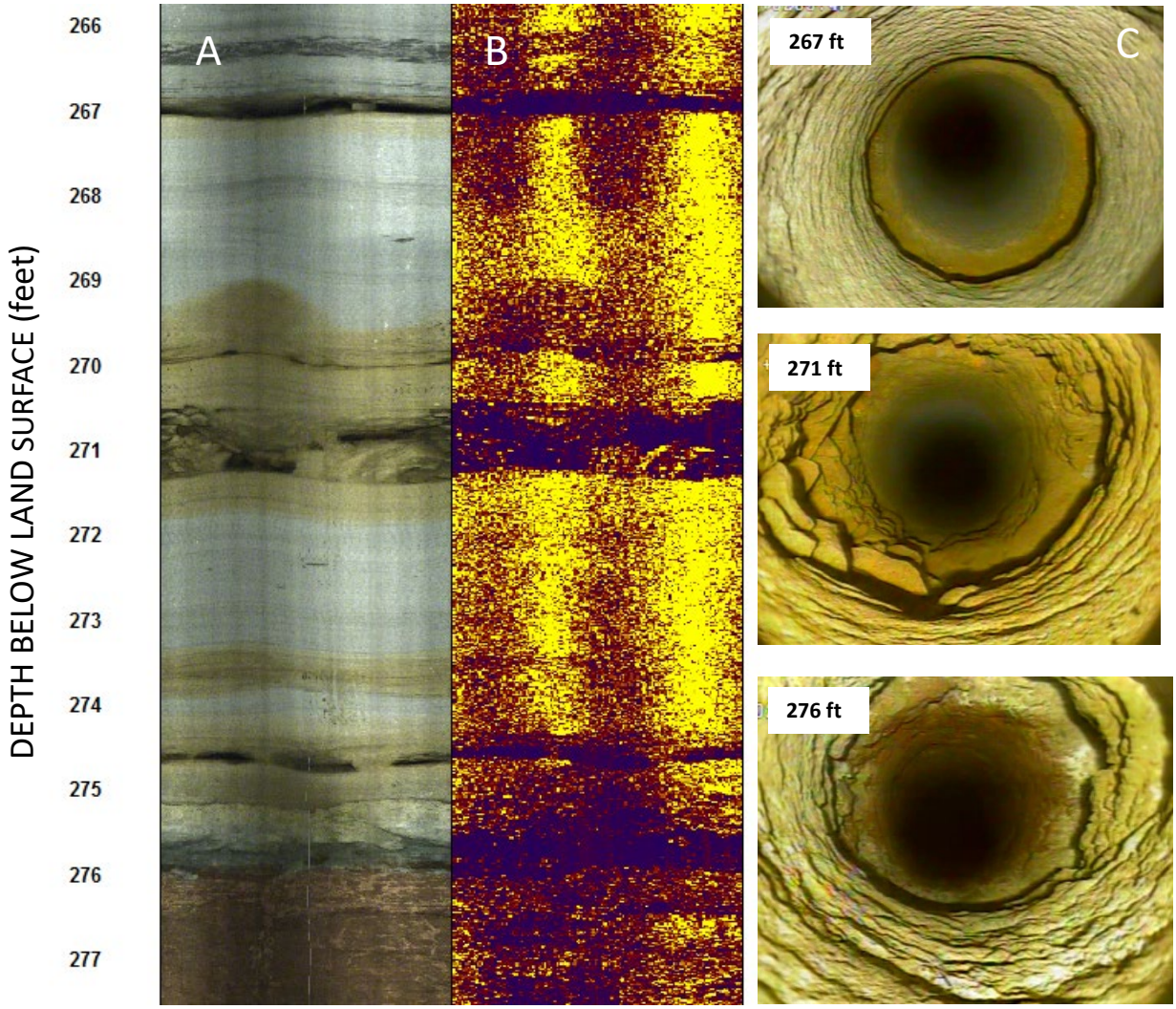

Figure 13. Water-bearing zone at 267–275 ft bls associated with bedding-related fractures in sandstone above a contact with red shale: A) optical-televiewer image, B) acoustic-televiewer image, and C) video images.

Fracture Zone 4—425 ft

The water-bearing zone at 425 ft bls was associated with two bedding-related fractures in sandstone as shown on image and video logs (Figure 14). During drilling, an increase in air-blown yield of about 30 gal/min was attributed to this zone, although a substantial amount of the increase may have been from further development of more transmissive fracture zones above as drilling progressed. After completion of the test hole, the fluid-flow logs showed that about 4.8 gal/min of the downflow exited at the zone under ambient open-hole conditions. This rate of outflow from the test hole was only slightly reduced when it was pumped at 16.2 gal/min. A change in slope on the temperature log also documents the water-bearing zone at this depth (Figure 10).

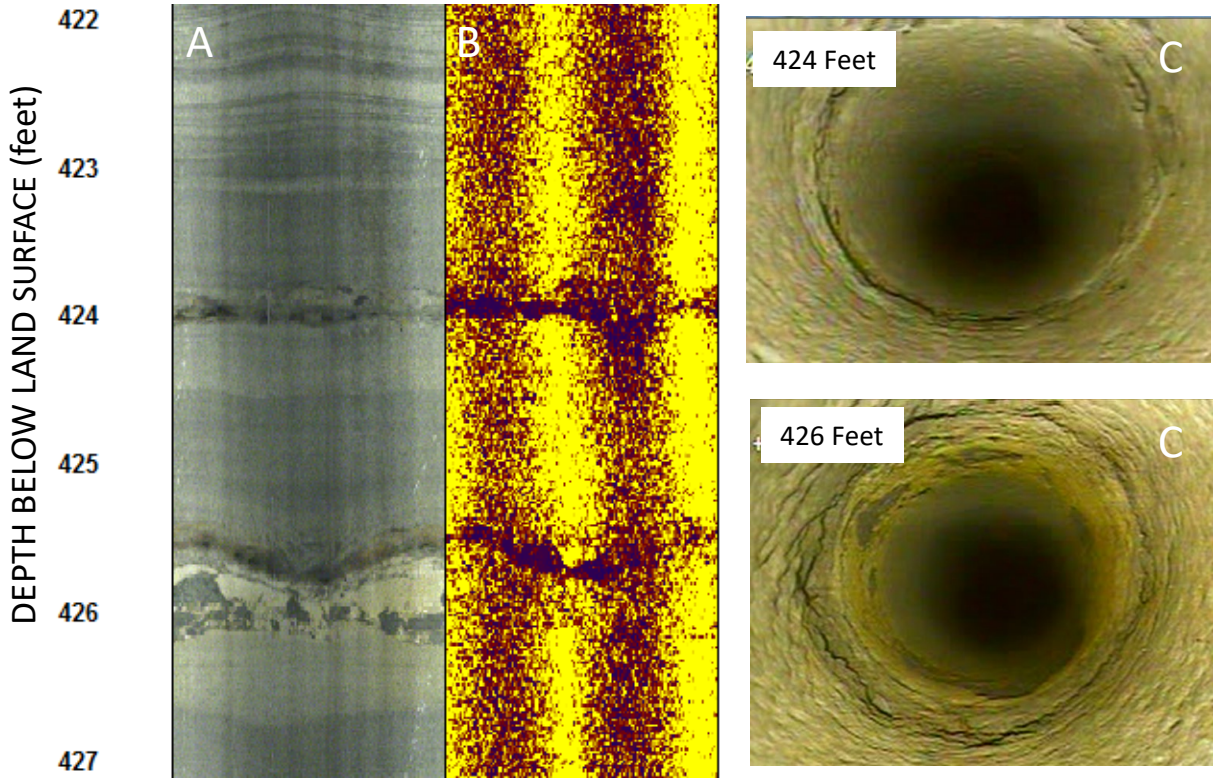

Figure 14. Water-bearing zone at 425 ft bls associated with bedding-related fractures in sandstone: A) optical-televiewer image, B) acoustic-televiewer image, and C) video images.

Fracture Zone 5—637 to 644 ft

The water-bearing zone at 637 to 644 ft bls was associated with multiple bedding-related and higher angle fractures in green sandstone as shown by an enlargement of the hole on the caliper log, large change in fluid resistivity and derived specific conductance, change in slope of fluid-temperature log (Figure 10), and on image and video logs (Figure 15). During drilling, the increase in air-blown yield attributed to this zone was 15 gal/min. After completion of the test hole, the fluid-flow logs showed that about 0.4 gal/min of water flow down the hole exited at this zone under ambient open-hole conditions. This rate of outflow was only slightly reduced when the open test hole was being pumped at 16.2 gal/min.

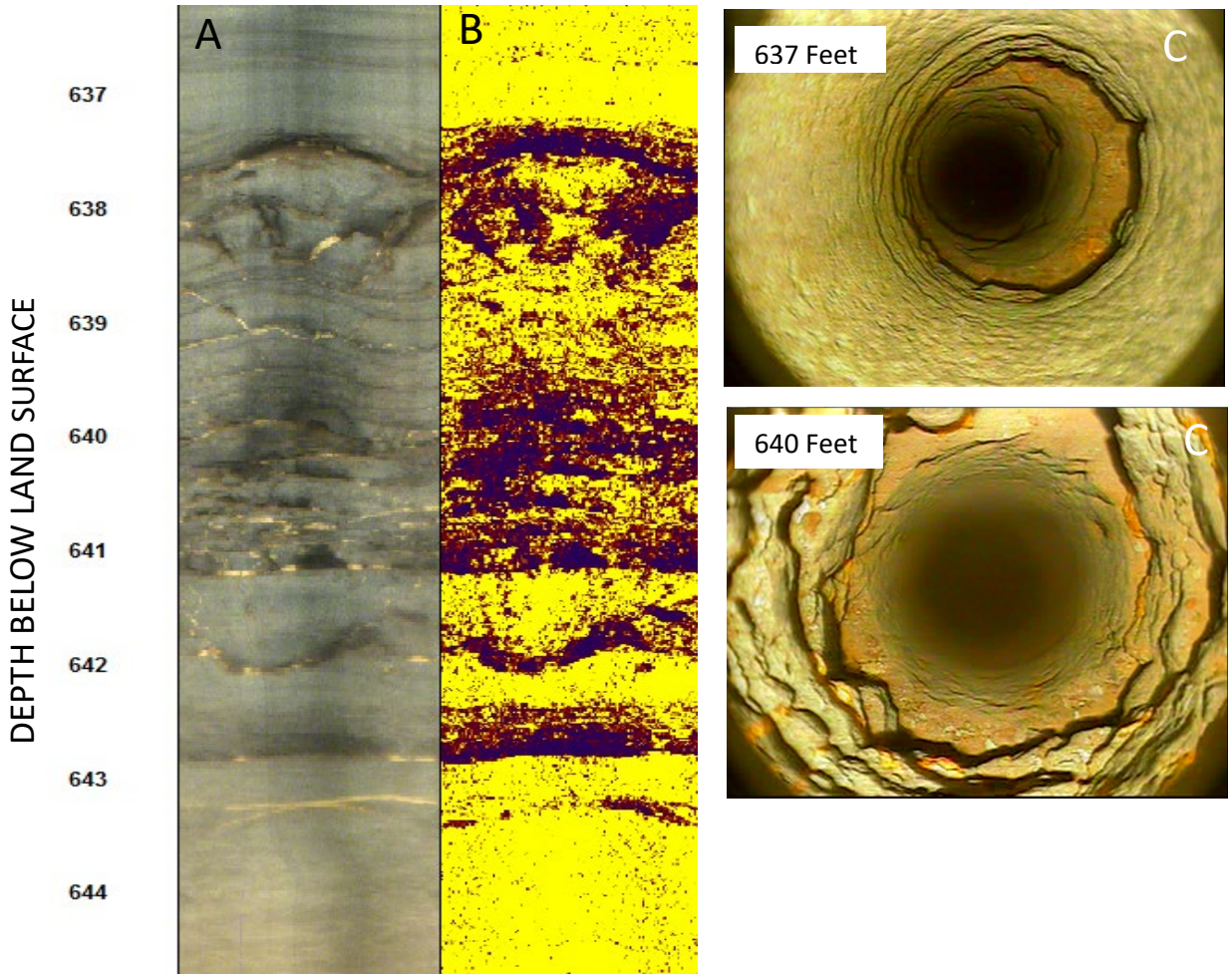

Figure 15. Water-bearing zone at 637 to 644 ft bls associated with multiple bedding-related and higher angle fractures in green sandstone: A) optical-televiewer image, B) acoustic-televiewer image, and C) video images

Fracture Zone 6—1,003 ft

No flow was detected by the flowmeter below the water-bearing zone at 637–644 ft bls, and the temperature gradient below that zone to the bottom of the test hole approached the geothermal gradient (Figure 10), indicating minimal fracture transmissivity in this interval. Also, the video log collected on July 30, 2013, showed poor visibility below 640 ft bls, indicating little vertical fluid flow within the test hole. A thin bedding fracture at 1,003 ft bls was associated with a very small inflow of saline water under ambient open-hole conditions as indicated by a large change in fluid resistivity and derived specific conductance at that depth (Figure 10). The saline-water inflow resulted in streaks of reddish iron-oxide staining extending below several distinct points along the bedding-related fracture as shown on the optical-televiewer log and video log collected on November 11, 2013, after the visibility in the hole had improved. The iron-oxide staining of the most prominent streak also extended above the fracture (Figure 16). Less prominent streaking also was seen on the video from several bedding-plane fractures at about 958 and 989 ft bls. The specific conductance of the saline inflow was 29,300 µS/cm at 25°C as indicated by the specific-depth sample collected at 990 ft bls on July 28, 2014. The time series of fluid-resistivity and specific-conductance logs collected between July 23, 2013, and July 28, 2014, indicated apparent downward and upward flow of the saline water. The slow downward movement of the saline water could be the result of the greater density of the saline-water inflow compared to the water in the test hole after drilling. Upward movement of saline water could be caused by diffusion or advection by rising methane-gas bubbles.

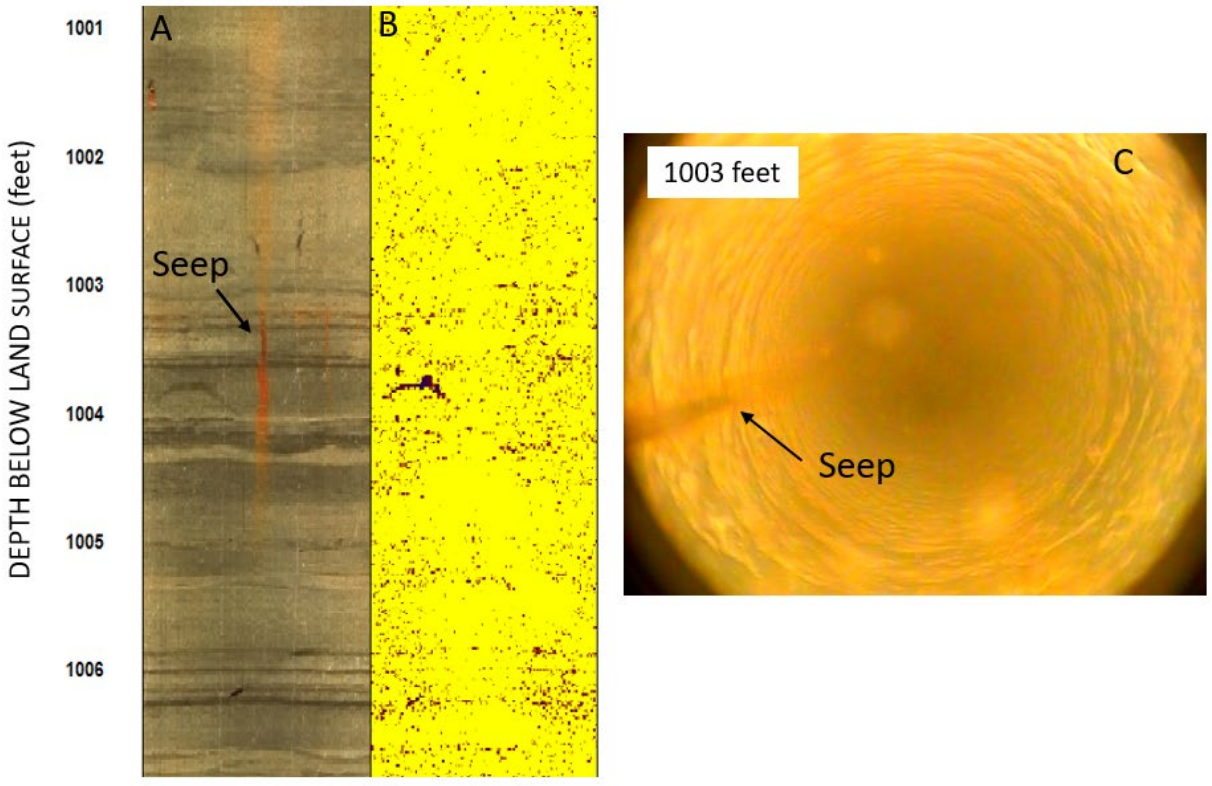

Figure 16. Bedding-related fracture at 1,003.2 ft bls associated with saline-water inflow: (A) optical-televiewer image, (B) acoustic-televiewer image, and (C) video image.

HYDRAULIC PROPERTIES

The hydraulic head, specific capacity, and transmissivity of the open-hole and individual fractured water-bearing zones penetrated by the test hole were characterized by water-level measurements, analysis of flow logs during ambient and pumping conditions, and by isolated-interval tests. The hydraulic properties of the open test hole and individual isolated water-bearing fractures penetrated by the test hole are presented in Figure 17 and are described below.

Open Hole

Hydraulic heads in the open 1,400-ft-deep test hole were determined from periodic measurements of the water level under static, ambient (non-pumping) conditions between July 2013 and July 2014. Water levels measured during that period fluctuated about 15 ft, ranging from a high of 131.0 ft bls on July 25, 2013, to a low of 146.27 ft bls on November 7, 2013. These water levels correspond to hydraulic heads of about 2,198 to 2,183 ft above sea level, respectively. The hydraulic head in the open test hole represents a composite of the hydraulic heads from the individual water-yielding fractures penetrated by the test hole.

The specific capacity of the open test hole was 3.9 (gal/min)/ft with a quasi-steady-state drawdown of 4.2 ft after pumping at 16.2 gal/min for approximately 1 hour. The total transmissivity of the test hole estimated from the specific-capacity data by iterative solution of Eq. 1 was 850 ft^2/d for the 8-inch diameter test hole and an assumed aquifer storage coefficient of 0.0005. The total transmissivity of the test hole estimated from the late-time drawdown data using the straight-line method of Cooper and Jacob (1946) was 440 ft^2/d (Figure 18), which was about half of the value from the specific-capacity estimate.

Water-Bearing Fracture Zones

Estimates were made of the hydraulic head, specific capacity, and transmissivity for five individual fractured water-bearing zones. The estimates were derived from open-hole flow-log analysis and by isolating zones with packers.

Open-Hole Flow-Log Analysis

Estimates of hydraulic head and transmissivity for individual water-bearing fracture zones were made by use of the computer model FLASH (Day-Lewis and others, 2011) for open-hole flow-logs collected on July 25, 2013. The values of hydraulic head and transmissivity of the individual water-bearing zones used in the FLASH model produce simulated vertical flows in the open hole that are compared to measured values from the flowmeter log for ambient and pumping conditions as shown in Figure 19.

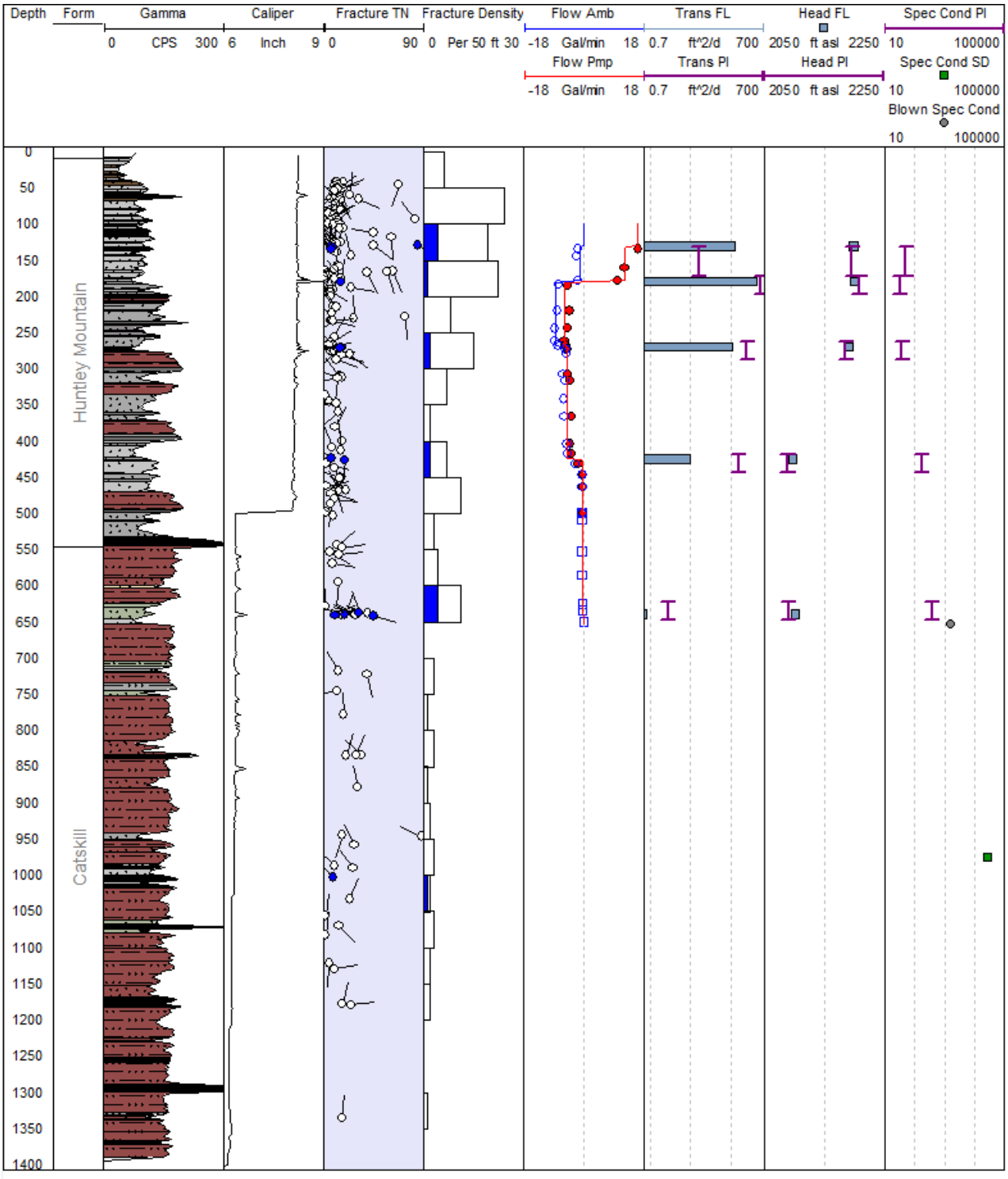

Figure 17. Logs of stratigraphy, lithology, gamma, caliper, fracture and water-bearing fracture orientation, and transmissivity, hydraulic head, and specific conductance of water-bearing zones in the Laporte test hole, Sullivan County, Pa. (Explanation of log headings, units, colors, and symbols are presented on pages x–xii).

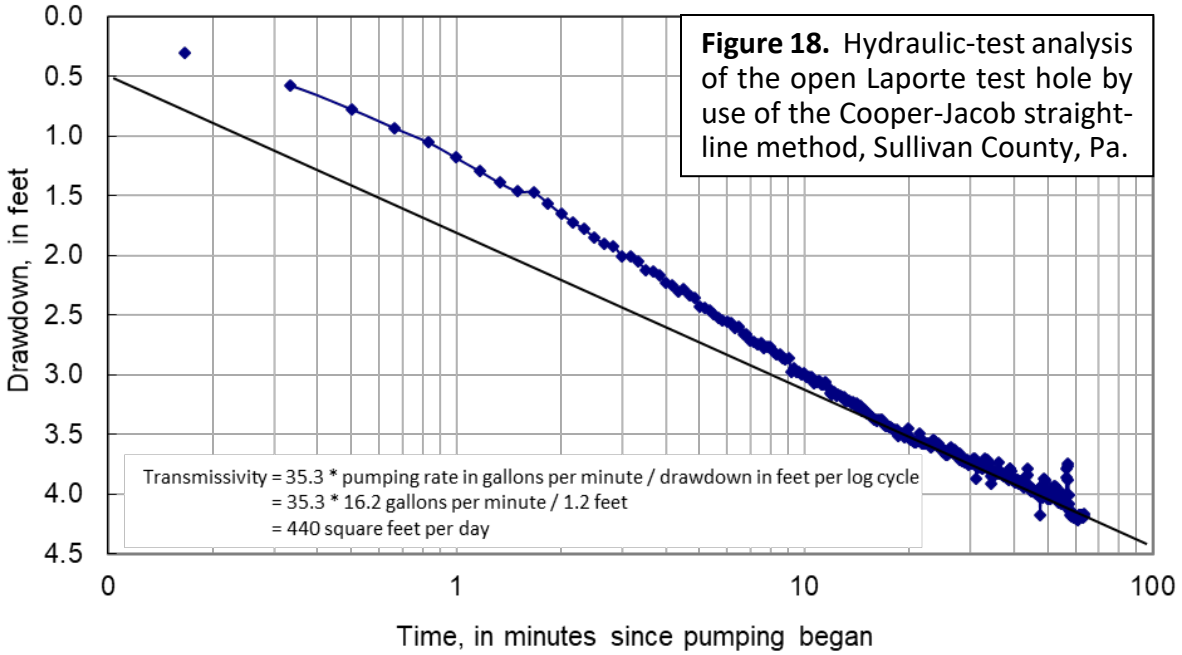

Figure 18. Hydraulic-test analysis of the open Laporte test hole by use of the Cooper-Jacob straight-line method, Sullivan County, Pa.

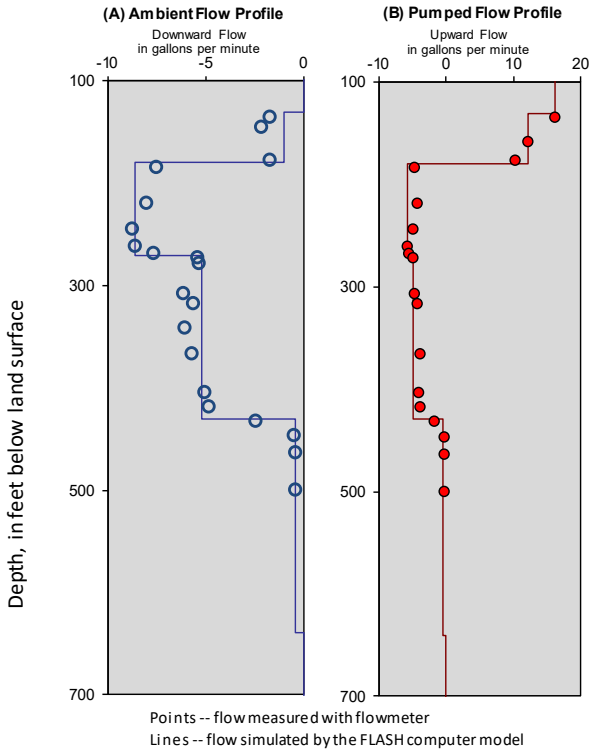

Figure 19. Analysis of open-hole flow with the FLASH model showing measured flow under (A) ambient and (B) pumping conditions compared to open-hole flow simulted with the FLASH model for estimated values of hydraulic head and transmissivity of individual fracture zones for the Laporte test hole, Sullivan County, Pa.

Water-bearing fracture zone	Depth of water-bearing fracture zone, in feet below land surface	Results from FLASH model				
		Water level of zone, in feet below land surface	Static head in open hole minus farfield head of zone, in feet	Altitude of farfield head, in feet above sea level	Transmissivity of zone [square feet per day]	Fraction of total transmissivity in zone
1	131	129.6	1.4	2199.4	160	0.19
2	180	127.9	3.1	2201.1	550	0.64
3	270	136.6	-5.6	2192.4	140	0.16
4	430	231.0	-100.0	2098.0	11	0.01
5	640	229.8	-98.8	2099.2	1	<0.01

Isolation of Intervals With Packers

Estimates of hydraulic head, specific capacity, and transmissivity for individual fractures were also made by isolating the fractured water-bearing zones with packers. Figures showing the water levels for the isolated interval and the intervals above and below the isolated interval are presented, and a summary of the results for each interval is provided below.

Isolated interval 1 (172 ft and above)—A single packer was set at a depth of 172 ft bls on August 6, 2013, to isolate the interval from that depth to the static water level of about 138 ft bls. The intent was to isolate the fractured water-bearing zone previously identified at 130–135 ft bls, but the water level was below those fractures at the time of the test though some water may have been cascading from 130–135 ft bls. The water level above the packer rose about 4.8 ft to 133 ft bls 47 minutes after packer inflation. The isolated interval was initially pumped at 15 gal/min, which drew the level down below the transducer setting and then below the pump after only about 6 minutes of pumping (Figure 20). The pump was shut off for 28 minutes, then was restarted and the interval was pumped for 68 minutes at 1.3 gal/min, during which a water sample was collected at 17:30 (Tables A1–A4). Specific capacity after 1 hour of pumping was about 0.07 (gal/min)/ft, and transmissivity estimated from this specific capacity value was about 12 ft^2/d.

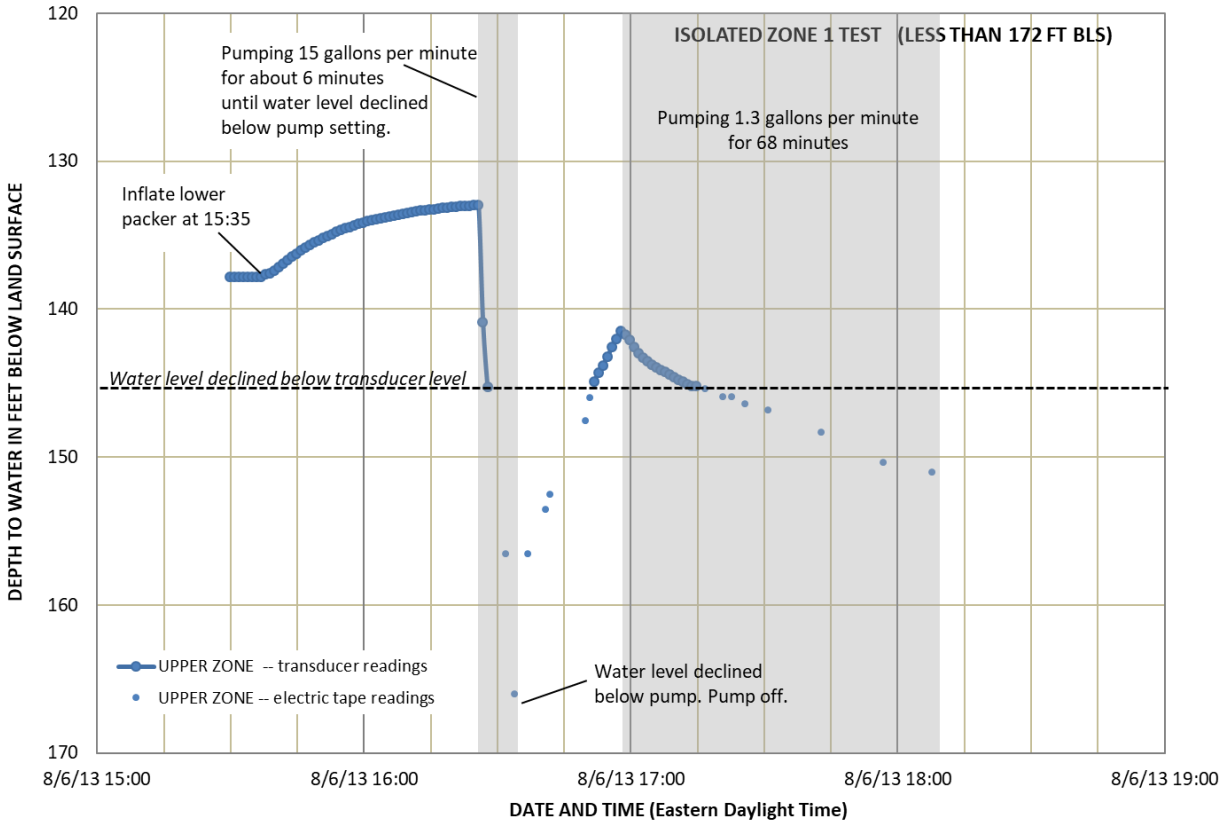

Figure 20. Water levels during the hydraulic test of isolated interval 1 from 137.8 to 172 ft bls in the Laporte test hole, Sullivan County, Pa.

Isolated interval 2 (172–197 ft bls)—Both packers were inflated the evening of August 6, 2013, to isolate the depth interval from 172 to 197 ft bls, which included the fractured water-bearing zone previously identified at 180 ft bls. The packers remained inflated overnight to allow for heads to equilibrate. The static water level was 137.9 ft bls prior to packer inflation. About 14 hours after inflation, the water level in the isolated interval had risen about 13.8 ft to 124.1 ft bls; the level in the upper interval had risen 17.3 ft, and the level in the lower interval had declined 17.3 ft (Figure 21). The isolated interval was pumped at 9.9 gal/min for 70 minutes. After 1 hour, the water level in the isolated interval declined 4.7 ft resulting in a specific capacity of 2.1 (gal/min)/ft. Transmissivity estimated from this specific capacity value was about 490 ft^2/d. During pumping, hydraulic heads in the upper and lower intervals declined very slightly. The decline in the lower interval was a continuation of the trend caused by packer inflation and does not indicate a connection with the pumped interval. The small water-level decline of about 0.25 ft in the upper interval is difficult to assess; because of an equipment malfunction only periodic measurements were made. The decline might be caused by a slight hydraulic connection to the isolated pumped interval. A water sample was collected on 8/7/13 (Tables A1–A4).

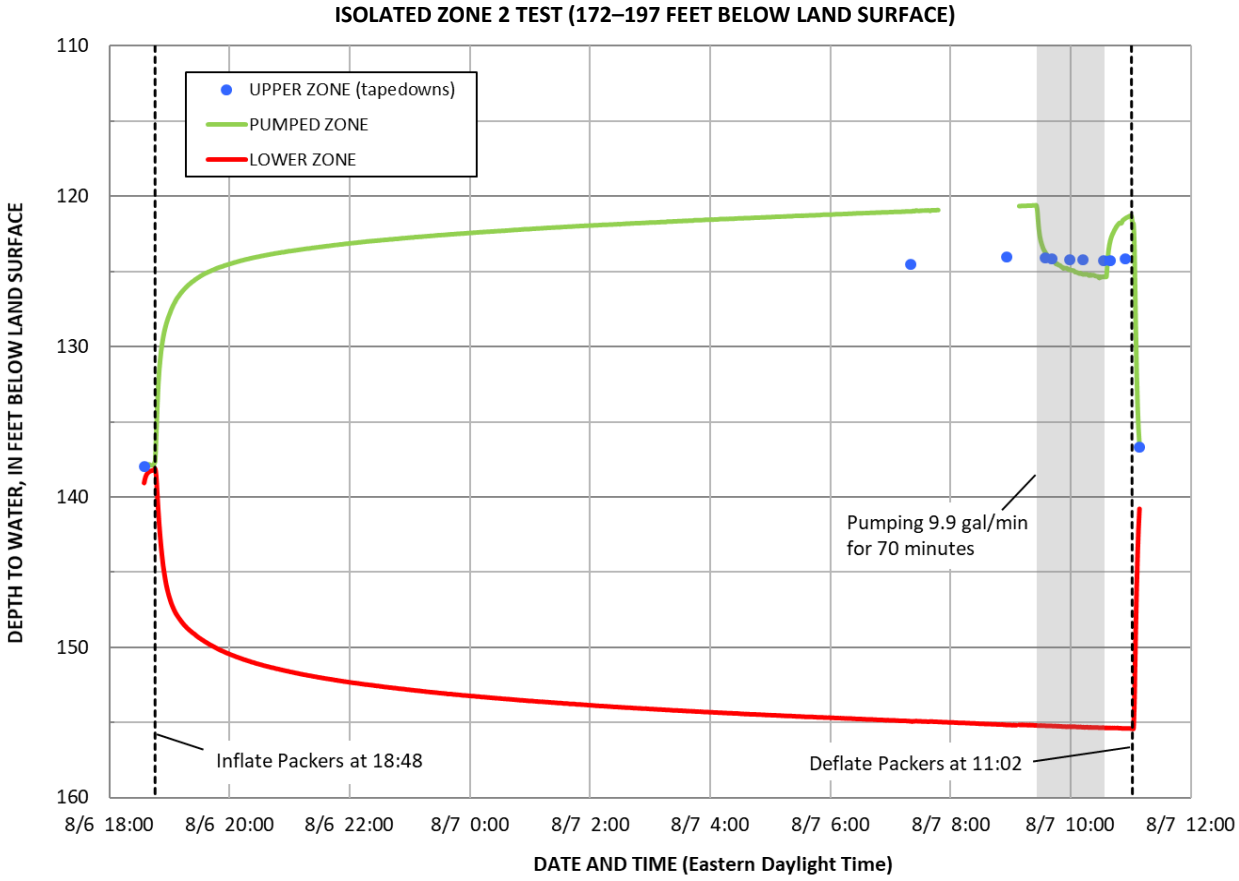

Figure 21. Water levels during the hydraulic test of isolated interval 2 from 172 to 197 ft bls in the Laporte test hole, Sullivan County, Pa.

Isolated interval 3 (263–288 ft bls)—Both packers were inflated the afternoon of August 7, 2013, to isolate the depth interval from 263 to 288 ft bls, which included the fractured water-bearing zone previously identified at 267–275 ft bls. The packers remained inflated overnight to allow for heads to equilibrate. The static water level was about 136 ft bls prior to packer inflation. About 15 hours after inflation, the water level in the isolated interval had declined about 8 ft to 144 ft bls; the level in the upper interval had risen 16 ft, and the level in the lower interval had declined about 68 ft. The level in the lower interval dropped below the transducer during equilibration, but the transducer was lowered before pumping began (Figure 22). The isolated interval was pumped on 8/8/13 for 108 minutes in steps of about 5, 8, and 12 gal/min. The average rate was about 10.6 gal/min.

After 1 hour, the water level in the isolated interval declined 10.4 ft resulting in a specific capacity of about 1.2 (gal/min)/ft for a pumping rate of 12 gal/min. Transmissivity estimated from this specific capacity value was about 220 square ft/day. During pumping, hydraulic head in the lower intervals declined as continuation of the trend caused by packer inflation and does not indicate a connection with the pumped interval. The water level in the upper interval increased about 0.85 ft, which probably indicates some leakage from the discharge tubing. A water sample was collected on 8/8/13 at 09:30 (Tables A1–A4).

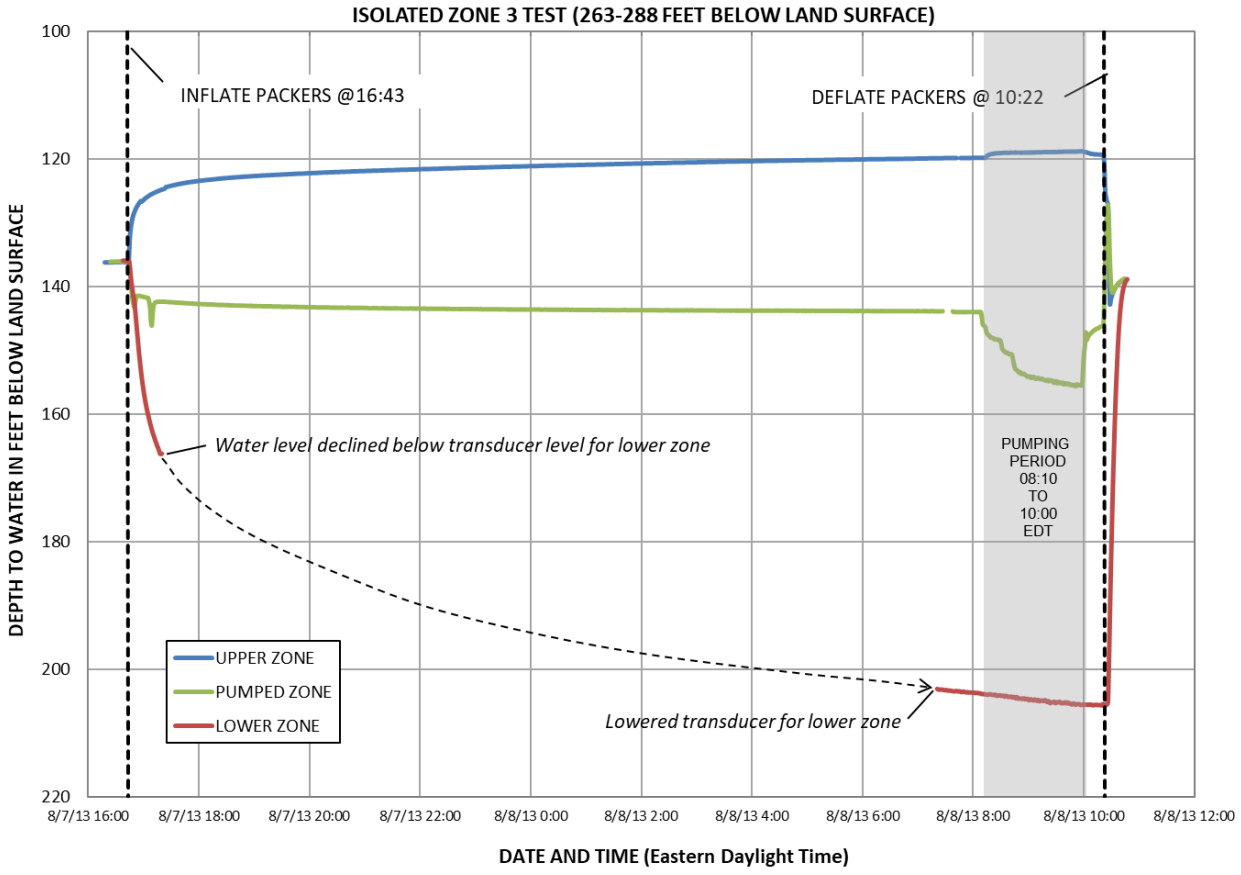

Figure 22. Water levels during the hydraulic test of isolated interval 3 from 263 to 288 ft bls in the Laporte test hole, Sullivan County, Pa.

Isolated interval 4 (418–443 ft bls)—Both packers were inflated the afternoon of August 8, 2013, to isolate the depth interval from 418–443 ft bls, which included the fractured water-bearing zone previously identified at 425 ft bls. The packers remained inflated for 2 hours to allow for heads to equilibrate. The static water level was about 136.3 ft bls prior to packer inflation. About 2 hours after inflation, the water level in the isolated interval had declined about 101 ft to 237 ft bls; the level in the upper interval had increased 4.5 ft, and the level in the lower interval declined about 44 ft (Figure 23). The level in the lower interval is not believed to be correct; it should be at or lower than the head in the isolated interval because the fluid conductivity log does not suggest any upward flow (Figure 10). Most likely, the access tubing used to monitor the lower interval was leaking from above the upper packer, causing the water level bls for the lower interval to be too high. The isolated interval was pumped on 8/8/13 for 218 minutes at a rate that declined from 8.6 to 7.7 gal/min. After 1 hour, the water level in the isolated interval declined 14 ft resulting in a specific capacity of about 0.56 (gal/min)/ft for a pumping rate of 7.9 gal/min. Transmissivity estimated from this specific capacity value was about 119 ft^2/d. During pumping, hydraulic head in the lower interval declined as a continuation of the trend caused by packer inflation and does not indicate a connection with the pumped interval. The water level in the upper interval increased about 0.85 ft, part of which was from a continuation of the pre-pumping trend caused by packer inflation. Because the field water-quality parameters did not stabilize during pumping, the chemical analysis of the water sample that was collected is not included in Tables A1–A4 because it is probably not representative of the isolated interval. The packers were left inflated in the test hole until August 12, 2013, at which time the isolated interval was again pumped at an average rate of 7.8 gal/min for about 85 minutes. Field parameters of the discharged water were stable at that time, so a sample was collected on August 12, 2013, at 10:55 (Tables A1–A4).

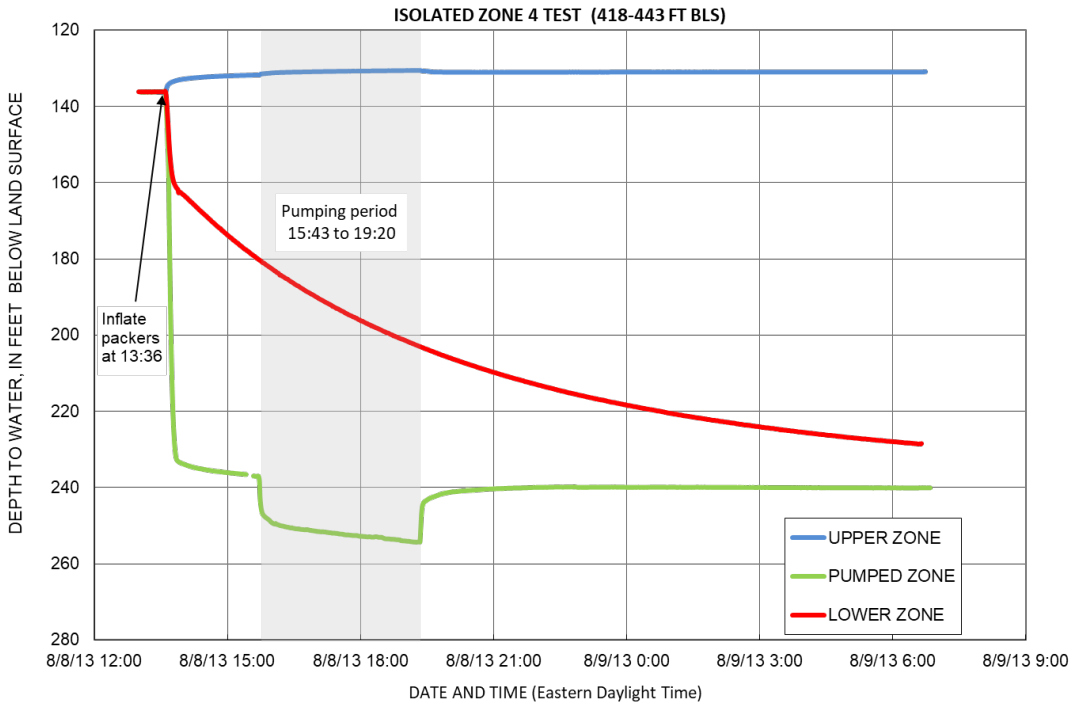

Figure 23. Water levels during the hydraulic test of interval 4 from 418 to 443 ft bls in the Laporte test hole, Sullivan County, Pa.

Isolated interval 5 (621–646 ft bls)—Both packers were inflated the late afternoon of August 28, 2013, to isolate the depth interval from 621 to 646 ft bls, which included the fractured water-bearing zone previously identified at 637–644 ft bls. The packers remained inflated for 15 hours to allow for heads to equilibrate. The static water level in the open hole was 138.3 ft bls prior to packer inflation. About 15 hours after inflation, the water level in the isolated interval had declined about 90 ft to 228 ft bls; the level in the upper interval had increased 0.2 ft, and the level in the lower interval declined about 1.9 ft (Figure 24). The level in the lower interval is not believed to be correct because in previous attempts to isolate this interval, leaks in the PVC access pipes were detected. Most likely, leaks in the access pipe used to monitor the lower interval had not been fixed; however, the head change in the packed-off interval indicates it has been isolated.

The isolated interval was pumped on 8/29/13 for 374 minutes at a rate that began at 1.3 gal/min and decreased to 0.8 gal/min during the first 310 minutes and was only about 0.3 gal/min during the last 64 minutes. The average rate was about 0.96 gal/min. After 1 hour, the water level in the isolated interval declined 93 ft resulting in a specific capacity of about 0.01 (gal/min)/ft for a pumping rate of 1.3 gal/min. Transmissivity estimated from this specific capacity value was about 1 ft^2/d.

During pumping, the water level in the upper interval increased about 0.82 ft, which probably indicates leakage from the discharge tubing. The water level in the lower interval declined 0.7 ft during the first hour and was 6.9 ft lower by the end of the test, indicating a hydraulic connection with the pumped interval. The field water-quality parameters did not stabilize during pumping, but a water sample was collected and analyzed (Tables A1–A4). The sample is probably not fully representative of the water from fractures in this depth interval because of the apparent hydraulic connection with the lower interval.

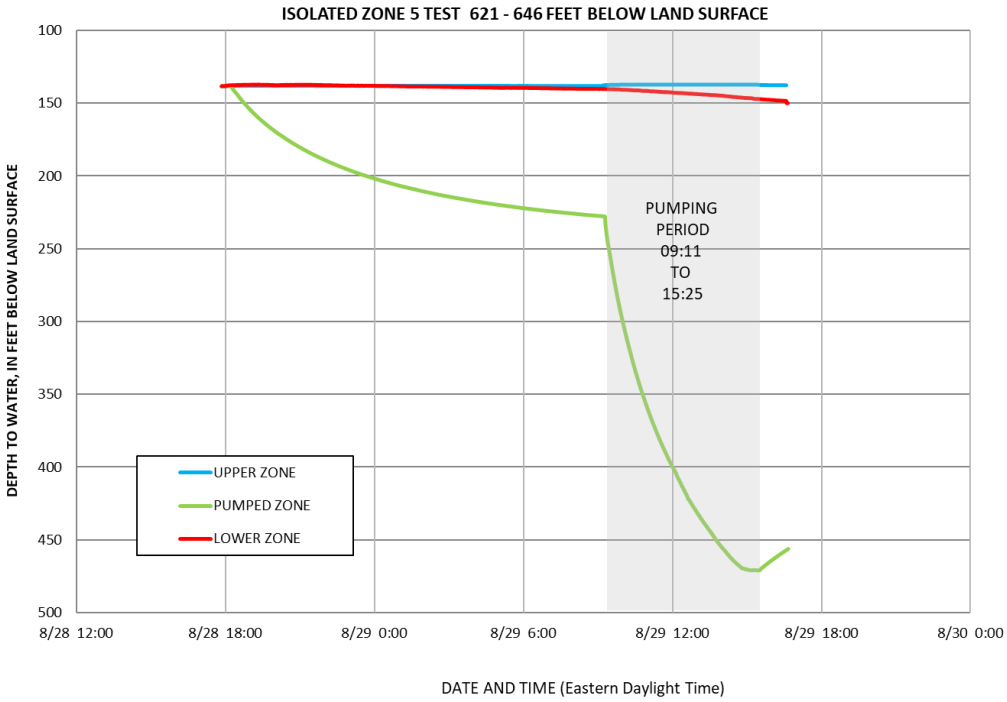

Figure 24. Water levels during the hydraulic test of interval 5 from 621 to 644 ft bls in the Laporte test hole, Sullivan County, Pa.

Summary of Hydraulic Properties

A summary of the observations for yield and estimates hydraulic properties are shown in Table 3. Differences in the results for the six water-bearing fracture zones are discussed below.

The hydraulic-head of the water-bearing fracture zone from 130–135 ft bls was 2,199 ft above sea level (asl) as estimated from the open-hole flow-log analysis and was 2,196 ft asl when measured after isolating with a single packer. These hydraulic heads were several ft higher than the contemporaneous composite head of the open test hole. The transmissivity of the water-bearing zone from 130–135 ft bls estimated from FLASH analysis of the open-hole flow logs was about 158 ft^2/d. This was much greater than the transmissivity of the fracture zone of 12 ft^2/d estimated from the specific capacity value of 0.07 gpd/ft after 1 hour of pumping from the interval isolated with a packer. Partial dewatering of the fracture zone that occurred between the open-hole logging and isolated-interval testing, as reflected by the declining open-hole water levels and the observed decrease in cascading water, is believed to account at least in part for the differences in estimates of transmissivity of this water-bearing zone.

The hydraulic head of the water-bearing fracture zone at 180 ft bls was 2,201 ft asl as estimated from the open-hole flow-log analysis and was 2,208 ft asl when measured after isolating the interval with packers. These hydraulic heads were 3 and 17 ft higher, respectively, than the contemporaneous composite head of the open test hole at the time of each test. This is consistent with ambient flow measurements in the open hole showing that this

Table 3. *Summary of air-blown yield, ambient flow, estimates of hydraulic properties, and dissolved-solids concentration of water-bearing fracture zones isolated by packers in the Laporte test hole, Sullivan County, Pa.*

[NAVD, North American Vertical Datum of 1988; mg/L, milligrams per liter; >, greater than]

Water-bearing fractured zone, in feet below land surface	Air-blown yield estimated at surface during drilling, in gallons per minute	From open-hole flow-log analysis on July 25, 2013			From analysis of pumping from zones isolated with packers during August 8-29, 2013			
		Ambient flow, in gallons per minute and direction	Estimated hydraulic head altitude, in feet above NAVD 88	Estimated transmissivity, in square feet per day	Hydraulic head altitude, in feet above NAVD 88	Specific capacity after 1-hour of pumping, in gallons per minute per foot	Transmissivity estimated from 1-hour specific capacity, in square feet per day	Total dissolved solids, in mg/L
ZONE 1 (130-135)	5	1 inflow	2,199	160	2,196	0.07	12	35
ZONE 2 (180)	100	>7 inflow	2,201	550	2,208	2.1	490	21
ZONE 3 (267-275)	20	3 outflow	2,192	140	2,185	1.0	220	28
ZONE 4 (425)	30	4.8 outflow	2,098	11	2,087	0.56	120	105
ZONE 5 (637-644)	15	0.4 outflow	2,099	1	2,099	0.01	1	209

fracture zone contributed more than 7 gal/min of downflow. The transmissivity of the water-bearing zone at 180 ft bls estimated from FLASH analysis of the open-hole flow logs was about 546 ft^2/d. This agreed closely to the estimate of transmissivity of 490 ft^2/d from the specific capacity value of 2.1 gpd/ft after 1 hour of pumping from the interval isolated with packers. Both analyses support the measurements of yield during drilling showing that this was the most productive of all the penetrated water-bearing zones. The results indicate that about 60 percent of the open-hole transmissivity is from this fracture zone.

The hydraulic head of the fractured water-bearing zone from 267–275 ft bls as estimated from the FLASH analysis of the open-hole flow-logs was 2,192 ft asl and was 2,185 ft asl when measured after the interval was isolated with packers. These hydraulic heads were about 6 to 8 ft lower than the contemporaneous composite head of the open test hole at the time of each test. This is consistent with ambient flow measurements in the open hole showing that these fractures received about 3 gal/min of downflow. The transmissivity of the water-bearing zone from 267–275 ft bls was 135 ft^2/d from analysis of the open-hole flow log and was about 221 ft^2/d as estimated from the specific capacity value of 1.0 gpd/ft after 1 hour of pumping from the interval.

The hydraulic head of the fractured water-bearing zone at 425 ft bls estimated from the FLASH analysis of the open-hole flow-logs was 2,098 ft asl and was 2,087 ft asl when measured after the interval was isolated with packers. These heads were about 100 ft lower than the contemporaneous composite heads in the open test hole at the time of each test. This indicates a large downward vertical hydraulic gradient and is consistent with ambient flow measurements in the open hole showing that this fracture zone received about 4.8 gal/min of downflow. The transmissivity of the 425-ft water-bearing zone was about 11 ft^2/d as estimated from analysis of the open-hole flow log and 119 ft^2/d as estimated from the specific capacity value of 0.56 (gal/min)/ft after 1 hour of pumping from the interval. Because the specific conductance of the discharged water did not stabilize during pumping on August 8, 2013, it is possible that leakage into the isolated interval during pumping may have caused the high estimate of transmissivity from the specific-capacity data.

The hydraulic head of the water-bearing zone from 637–644 ft bls was 2,099 ft asl estimated from the FLASH open-hole flow-log analysis and was 2,099 ft asl when measured after the interval was isolated with packers. These heads were about 100 ft lower than the contemporaneous composite heads of the open test hole. This is consistent with ambient flow measurements in the open hole showing that these fractures received about 0.4 gal/min of downflow. The transmissivity of the fracture zone at 637–644 ft bls was less than 1 ft^2/d as estimated from analysis of the open-hole flow log and was 1 ft^2/d as estimated from the specific capacity value of 0.01 (gal/min)/ft after 1 hour of pumping from the interval.

The hydraulic head values of water-bearing fractures at depths greater than 644 ft bls are difficult to determine because the fracture transmissivities of the fractures are so small. The head for the interval below 644 ft had not equilibrated when the 637–644 ft fracture zone was isolated with packers, but it appeared that the head might be higher for the interval below 644 ft than in the zone from 637–644 ft bls. The successive increases in specific conductance in the interval from 644 to 1,003 ft bls also suggest a possible upward hydraulic gradient causing slow advection of saline water from the fracture at 1,003 ft to the fractured water-bearing zone at 637–644 ft bls (Figure 10).

WATER-QUALITY CHARACTERIZATION

Changes in the chemical quality of water in the test hole with depth were investigated in a multistep approach. Initial indications of water quality were determined by analysis of specific-conductance measurements during drilling. After drilling was complete, geophysical logs of fluid resistivity and flow identified six fracture zones where water entered or exited the test hole. Differences in dissolved-solids concentration of transmissive zones that contributed flow were identified. Finally, five transmissive fracture zones were isolated with packers to a depth of 646 ft bls and water-quality samples were pumped from specific depths; water representing inflow from the sixth fracture zone was sampled at 990 ft bls with a depth-specific point water sample from the open test hole. Results of the chemical analyses are in Tables A1–A4 in the appendices of this report.

SALINITY

The salinity of water in the test hole was characterized indirectly by measurements of specific conductance and fluid resistivity and directly by laboratory analysis of total dissolved solids. These measurements were made first for water returns during drilling, then by analysis of geophysical logs and collection of depth-specific samples.

Measurements During Drilling

The specific conductance of the water blown to the surface with the rock cuttings during drilling provided an initial indication of changes in water quality with depth. The water that returned to the surface was a mixture of water yielded from the rocks and water added by the driller. The specific conductance of the water added by the driller was very low to less than 20 μS/cm at 25°C. Specific conductance of water blown during drilling from 132 to 492 ft bls ranged from 36 to 226 μS/cm at 25°C (Figures 10 and 25). When drilling reached 500 ft bls, the hole was cased to block off the water inflow. Water did not return to the surface during drilling from 500 to 630 ft bls. Below 630 ft, the specific conductance of the blown water, although highly variable depending on how much drilling water was mixing with formation water in the sample, was much greater than in the upper part of the hole. Specific conductance from 631 to 1,400 ft bls ranged from 310 to 1,910 μS/cm at 25°C. The water-bearing fracture zone from 637–644 ft bls appeared to yield water with specific conductance ranging from about 1,350 to 1,910 μS/cm at 25°C. Assuming the blown water is mixed with the fresh drilling water to some extent, the best estimate of specific conductance for the water-bearing fracture zone from 637–644 ft bls is probably close to the highest reading—about 1,900 μS/cm at 25°C. The variable specific-conductance values below 650 ft bls probably represent water from the fractured zone at 637–644 ft mixing in various ratios with water added by the driller.

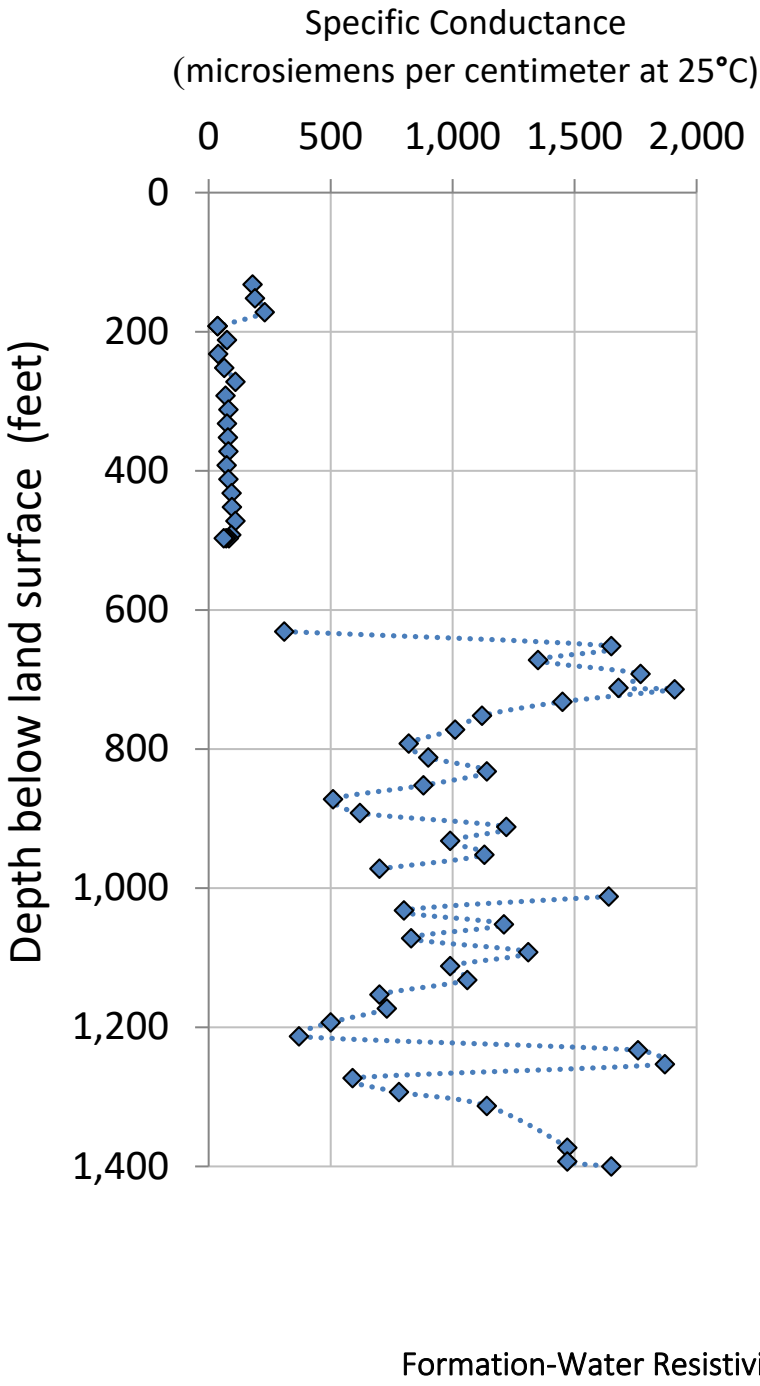

Figure 25. Specific conductance of water returns with cuttings to land surface during drilling of the Laporte test hole, Sullivan County, Pa.

Below a depth of 660 ft bls, the induction-conductivity and induction-resistivity logs, respectively, showed a significant increase and decrease relative to the gamma log. Shaded overlays of the induction-conductivity and induction-resistivity logs with the gamma log highlight this change (Figure 26). The increase in the induction-conductivity log values and decrease in the induction-resistivity log values relative to the gamma log values suggest an increase in the dissolved-solids content of the formation water.

Formation water resistivity was estimated for sandstone intervals with gamma values of less than 80 counts per second through application of Archie's Equation (Archie, 1942). Archie's Equation is an empirical relation that states:

$$R_w = R_t \, Ø^m \qquad \text{Eq. 3}$$

Where:
R_w is formation water resistivity (ohm-m),
R_t is true formation resistivity (ohm-m),
Ø is porosity (decimal),
m is cementation factor (dimensionless).

Values of true formation resistivity were derived from the induction resistivity log (Figure 26). Values of porosity were derived from the neutron porosity log, which is affected by not only the porosity of the formation but also its clay content. A cementation factor of 2.0, which is typical for consolidated sandstone, was assumed (Jorgensen and Petricola, 1994; Rider and Kennedy, 2011).

The application of Archie's Equation to estimate water quality is complicated by the variable clay content, presence of very fresh formation water in shallower intervals, low primary porosity, and discrete fractured nature of the bedrock. Because of the effects of surface conduction, Archie's Equation becomes invalid in a low-clay sandstone when fluid resistivity is greater than about 10 ohm-m (Hearst and Nelson, 1985). An increasing clay content increases surface conduction and lowers this threshold. The estimated formation water resistivities for the selected sandstone intervals above 450 ft bls generally ranged from 5 to 20 ohm-m (Figure 26). Between 450 to 900 ft bls, the estimated formation water resistivities generally ranged from 1 to 5 ohm-m. Below 900 ft bls, the estimated formation water resistivities generally were less than 1 ohm-m. A formation water resistivity of less than 1 ohm-m at the ambient formation temperatures of 10 to 15 degrees Celsius, as indicated by the temperature logs, corresponds to a specific conductance of more than 12,200 to 13,300 μS/cm at 25°C. The apparent transition from fresh to saline formation water between 450 and 900 ft bls that was estimated using this petrophysical approach is consistent with the fracture zones at 425, 637–644, and 1,003 ft bls being freshwater, transitional, and saline water-bearing zones, respectively.

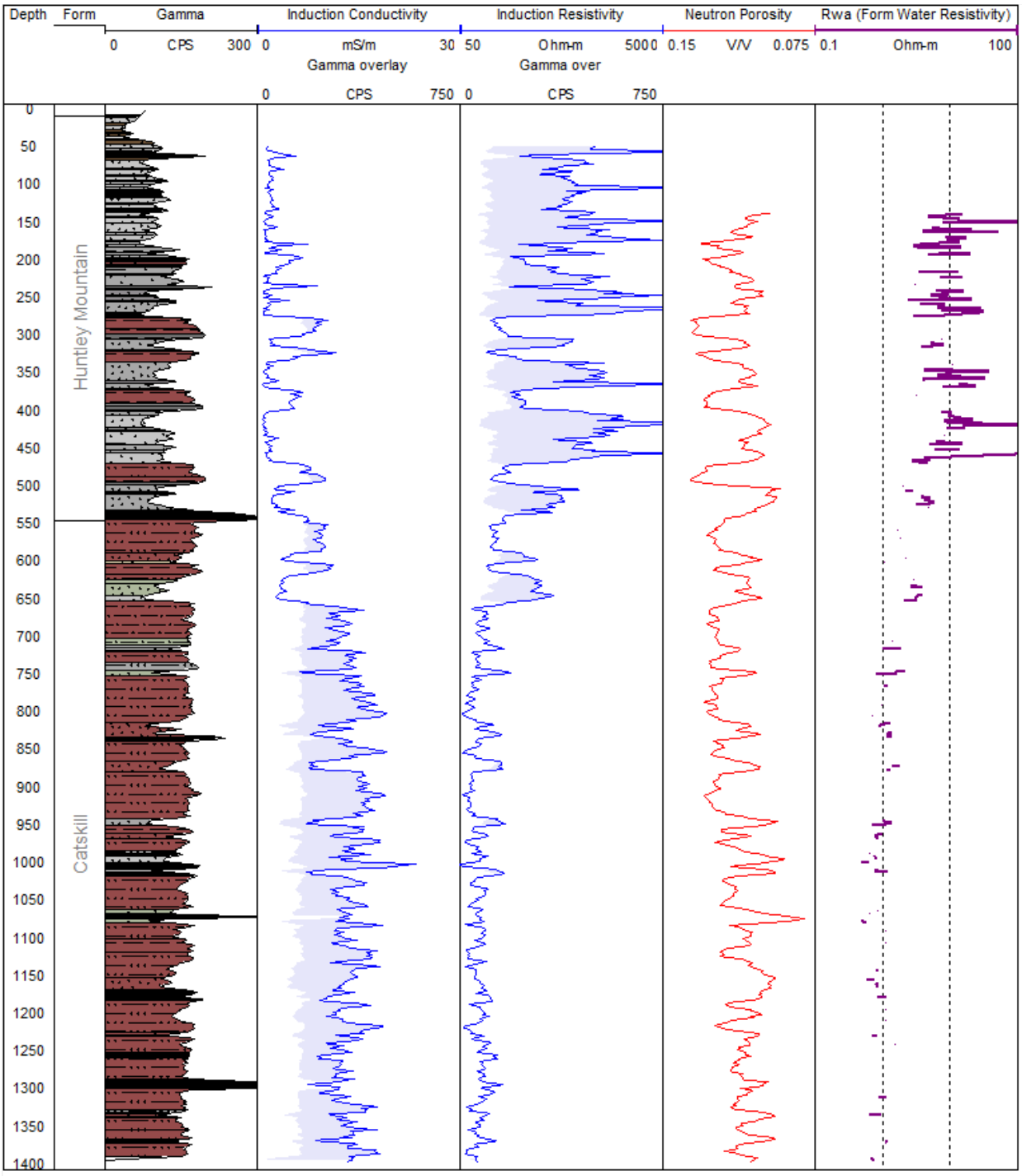

Figure 26. Logs of stratigraphy, lithology, gamma, induction conductivity, induction resistivity, neutron porosity, and estimated formation water resistivity for selected sandstone intervals in the Laporte test hole, Sullivan County, Pa. (Shading of induction-conductivity and induction-resistivity logs relative to gamma log. Explanation of log headings, units, and symbols are presented on pages x–xii.)

Depth-Specific Samples

Water samples were collected from the five fractured water-bearing zones to a depth of 644 ft bls that were isolated by packers (Table 2) during August 6–29, 2013. Additional depth-specific samples were collected in the open test hole at 990 ft bls by use of the point sampler on September 5, 2013, and July 28, 2014.

The dissolved-solids concentrations of water samples collected from three fracture zones from 130 to 275 ft bls that were isolated by packers were very low, ranging from 21 to 35 mg/L (Table A1). The concentration of dissolved solids in the sample from the water-bearing fracture at 425 ft bls was greater (105 mg/L) but could be categorized as freshwater because the dissolved-solids content is less than 1,000 mg/L (U.S. Geological Survey, 2019c). The dissolved-solids concentration of the water sample from fractures at 637–644 ft bls was 209 mg/L, but that value is probably not representative of the water-bearing zone because the specific conductance measured during purging of the interval continuously increased and had not stabilized after 4 hours of pumping. A better estimate of the dissolved-solids concentration of water from fractures at 637–644 ft bls is probably about 1,100 mg/L, derived as 60 percent of the highest specific-conductance value of the blown water shown on Figure 25 near that depth during drilling, which was 1,900 μS/cm at 25°C.

The dissolved-solids concentration of the deepest sample at 990 ft bls was 7,800 mg/L on September 5, 2013, and 19,900 mg/L when sampled on July 28, 2014. In contrast to the shallower freshwater samples, these deeper samples were moderately to highly saline (Figure 27). The concentration increased because the water in the open test hole at that depth was a mixture of the small seep of highly saline inflow from the fracture at about 1,003 ft bls with freshwater having specific conductance of less than 20 μS/cm at 25°C (dissolved solids probably less than 6 mg/L) initially added by the driller to flush the test hole after drilling. The water in the deep part of the hole below about 650 ft bls was made more saline over time by the inflow of the highly saline seepage from 1,003 ft bls. From the time-series of specific-conductance logs (Figure 10), it appears unlikely that the test-hole water column had reached equilibrium on July 28, 2014; thus, water from the seep at 1,003 ft bls is probably more saline than indicated by the samples.

Alley (2003) points out that definitions of saline water are somewhat arbitrary because water with dissolved solids in excess of 1,000 mg/L is used for drinking supply where better supplies are not available, but water with dissolved solids in excess of 3,000 mg/L is generally too salty to drink. The secondary maximum contaminant level for dissolved solids in drinking water is 500 mg/L (Pennsylvania Department of Environmental Protection, 2006; U.S. Environmental Protection Agency, 2009). For Pennsylvania streams having designated uses for public water supply (PWS) or coldwater fisheries (CWF), the general criteria for total dissolved-solids concentration is 500 mg/L as a monthly average value, with a maximum of 750 mg/L (Commonwealth of Pennsylvania, 2014).

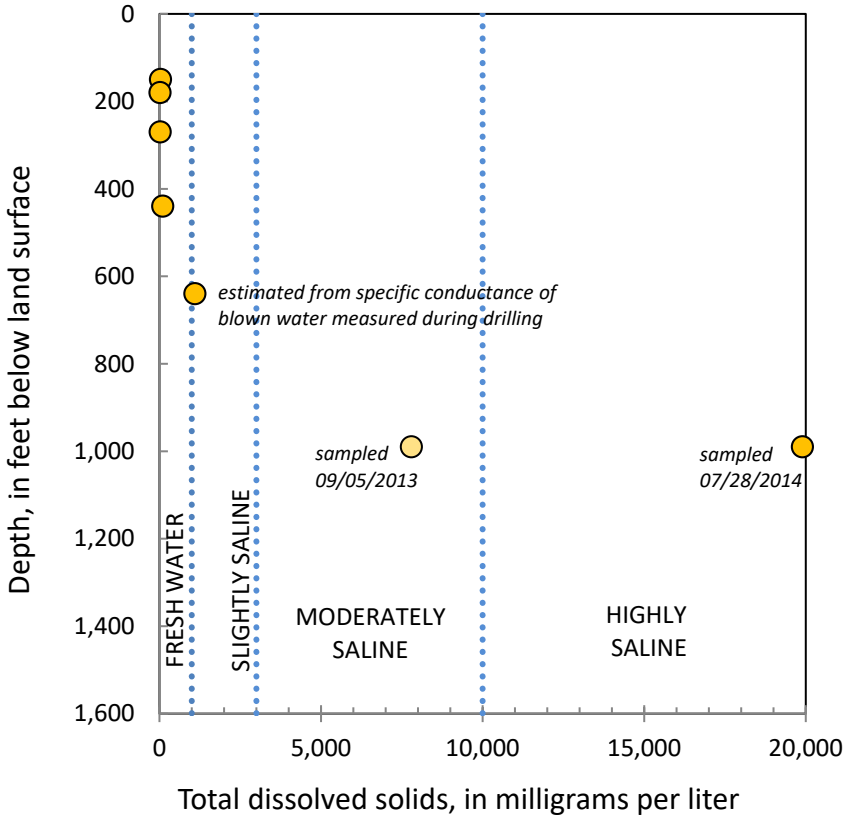

Figure 27. Total dissolved-solids concentration and designation of salinity of the water for samples collected at selected depths in the Laporte test hole, Sullivan County, Pa. Definitions of fresh and saline water are from U.S. Geological Survey (2019c).

MAJOR IONS

The major-ion composition of water samples from the Laporte test hole differed with depth as illustrated on a trilinear diagram (Figure 28). The predominant ions are calcium and bicarbonate in the four freshwater samples collected from isolated fractures at depths of 425 ft or less (Table A1). The predominant ions are sodium and chloride in the two moderately to highly saline water samples collected at 990 ft bls, with lesser amounts of calcium. For comparison, the compositions of some other saline waters are plotted on Figure 28. The relative percentages of major ions from the Laporte test hole at 990 ft bls are nearly identical to the water discharging at Salt Spring in Salt Spring State Park in Susquehanna County sampled by Warner and others (2012) and are similar in composition to oil- and gas-well brines in western Pennsylvania reported by Dresel and Rose (2010).

The major-ion chemistry of the sample from fractures at 637–644 ft bls differed from the waters in the test hole above and below (Figure 28). The sample was a sodium-bicarbonate-chloride water, but it is not a simple mixture of the shallow calcium-bicarbonate water with the deep sodium-chloride water. A mixture would plot in a straight line between the shallow calcium-bicarbonate samples (blue symbols) and deep sodium-chloride samples (red symbols) on the diamond plot in Figure 28, which it does not. The composition of the sample from fractures at 637–644 ft bls has a greater concentration of sodium than expected for a mixture. The extra sodium is probably the result of shallow calcium-bicarbonate recharge water exchanging calcium ions for sodium ions as it moves downward through shales in the

Catskill Formation. The water is transitional between the shallow sodium-bicarbonate freshwater samples and deep sodium-chloride saline-water samples. The chemical evolution for groundwater of similar composition from Wayne County, PA was modeled by Senior and others (2017).

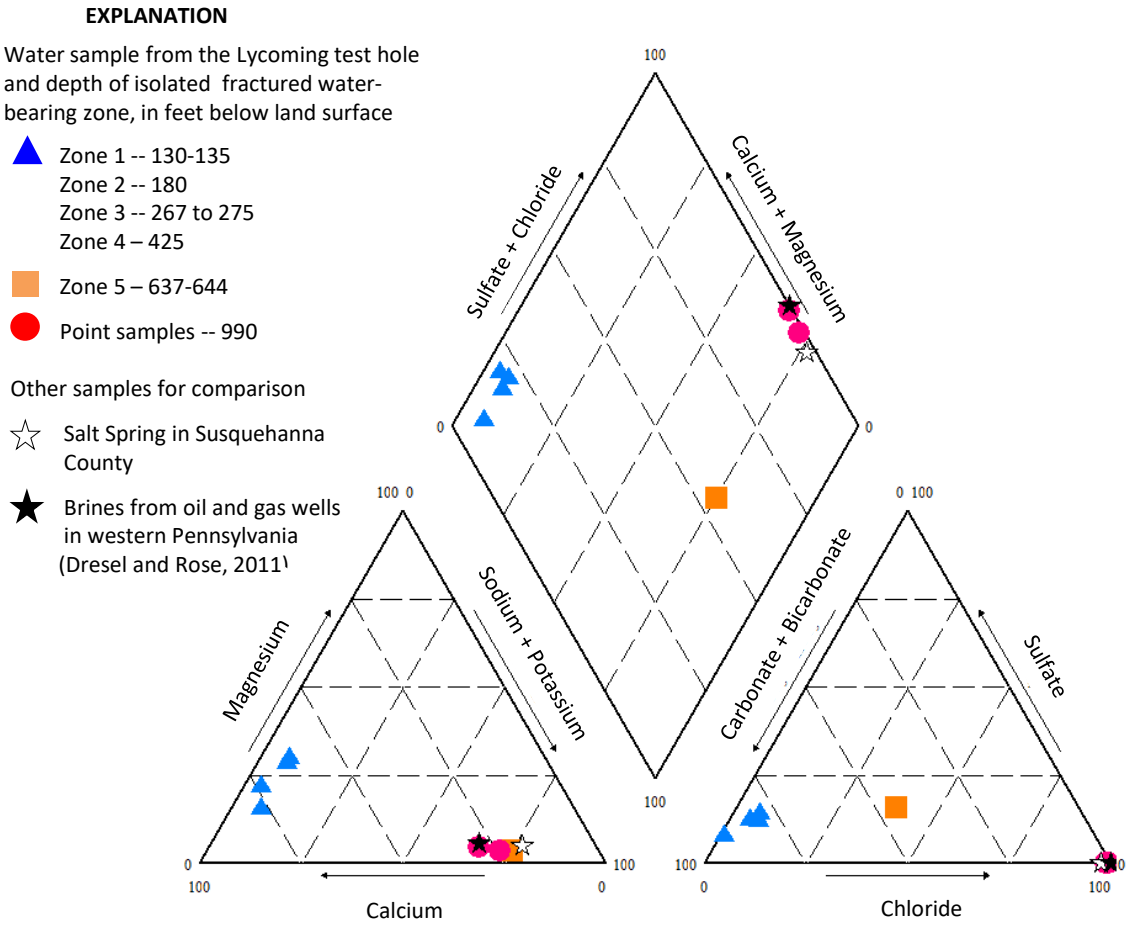

Figure 28. Trilinear diagram depicting the major-ion composition of eight depth-dependent water samples collected from the Laporte test hole, Sullivan County, Pa.

TRACE CONSTITUENTS AND RADIOCHEMICALS

Concentrations of trace constituents, gross alpha radioactivity, gross beta radioactivity, and radon analyzed in filtered water samples from the Laporte test hole are listed in Table A2. The trace constituents sampled from isolated fracture zones at 130–135, 180, 267–275, 425, and 637–644 and from a point sample at 990 ft bls are plotted in Figure 29. The trace metals are arranged on the x-axis of the graph in order of largest to smallest concentrations that were present in the highly saline sample from 990 ft bls on July 28, 2014. A few constituents detected at concentrations less than the reporting level are plotted at their reporting levels; those results can be found in Table A2.

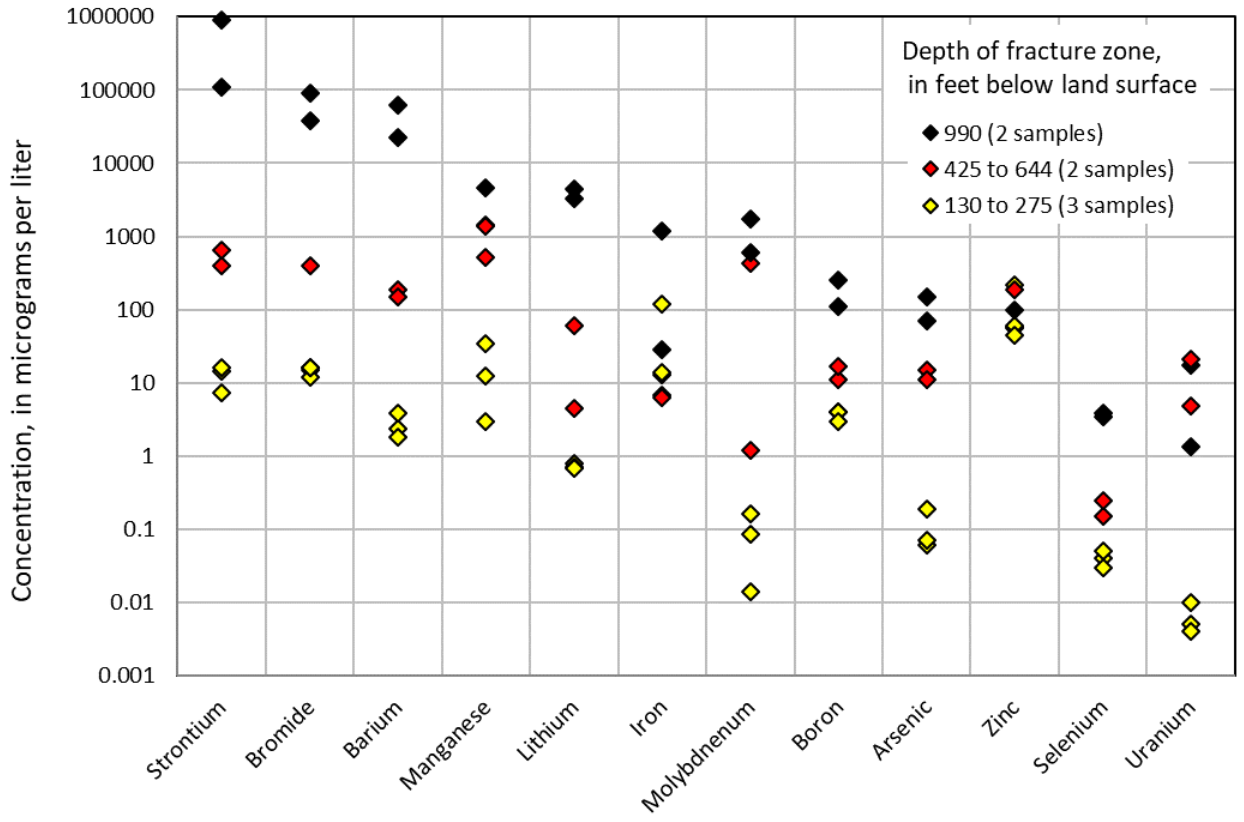

Figure 29. Concentrations of metals and other trace constituents in water sampled from specific depths between 167 and 990 ft bls in the Laporte test hole, Sullivan County, Pa.

The two moderately and highly saline water samples from 990 ft bls had higher concentrations of trace constituents than the freshwater samples from depths equal or less than 644 ft bls, except for zinc and uranium. The highest zinc concentration of 220 μg/L was in the sample from the fracture zone at 130–135 ft bls and the highest uranium concentration of 21.4 μg/L was in the sample from the fractures at 637–644 ft bls. Samples from intermediate fracture zones at 425 and 637–644 ft bls generally had trace-metal concentrations that were between those found in the shallow and deep samples. Some trace concentrations were especially elevated in the saline water samples from 990 ft bls relative to the freshwater samples from fractures between 130 and 275 ft bls. Concentrations of strontium, bromide, barium, lithium, and molybdenum were all more than 5,000-times greater in the sample from 990 compared to the sample having the lowest concentration from fractures at 130–135 or 180 ft bls. Barium was present in the sample from 990 ft bls at 30 times the primary maximum contaminant level (MCL) for drinking water of 2 mg/L, and arsenic was present at 15 times its MCL of 10 μg/L (U.S. Environmental Protection Agency, 2009).

Chloride and bromide tend to be conservative constituents in groundwater that, once dissolved, are not easily lost from solution by precipitation, ion exchange, or other reactions (Davis and others, 1998). Thus, they are commonly used as tracers and indicators of dilution or mixing of waters, provided that the concentrations in the end-member waters differ. Mixing of waters causes a change in concentration of bromide or chloride in direct proportion

to the mass loading from each end member. In the Laporte test hole, the ratio of chloride to bromide fits on the theoretical mixing curve between freshwater and brine (Figure 30), indicating that the source of elevated chloride in the sample is from saline porewater within the Catskill Formation. Based on the chloride concentrations, the sample from fractures at 637 to 644 ft bls appears transitional between the shallow freshwater samples from fractures at 130 to 425 ft bls and the saline samples from 990 ft bls.

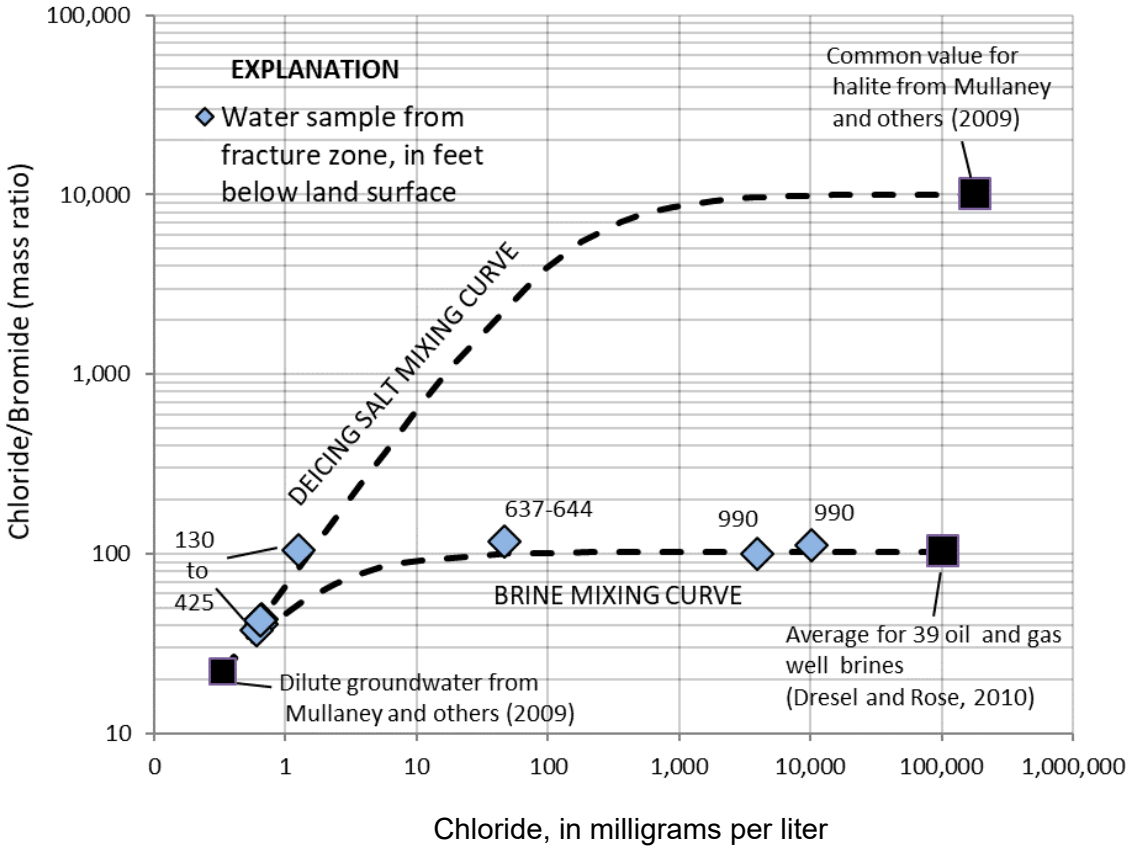

Figure 30. Relation between bromide and chloride concentrations in groundwater samples from 167 to 990 ft bls in the Laporte test hole, Sullivan County, Pa.

Mixing of the groundwater from 990 ft bls from this upland setting with dilute groundwater would result in chloride/bromide ratios falling along the brine mixing curve that would be difficult to distinguish from theoretical mixtures of freshwater with brines from the oil and gas fields. This could complicate efforts to distinguish freshwater that has been contaminated by brine from leaking gas wells from freshwater that has mixed with naturally occurring saline water from moderate depths of 990 ft bls.

Radiochemical analyses indicated that gross-alpha radioactivity exceeded the drinking water MCL of 15 pCi/L in samples from fractures zones at 637 to 644 and 990 ft bls. Gross alpha- and beta-particle activities are measures of the radioactivity in a water sample attributable to the decay of alpha- or beta-emitting elements, respectively. Because of the high concentration of total dissolved solids, concentrations of radium-226 could not be analyzed,

but they probably were elevated based on the high gross-alpha counts. The radium-228 value of 24.1 picocuries per liter (pCi/L) alone from 990 ft bls exceeds the drinking water MCL of 5 pCi/L (U.S. Environmental Protection Agency, 2009) for radium-226 plus radium-228 activity (Table A2). Radon concentrations are greatest (1,330 to 1,560 pC/L) in the shallow samples from fracture zones at 130 to 135 and 180 ft bls, where radium and uranium concentrations in water were smallest.

DISSOLVED GASES AND STABLE ISOTOPES

The concentrations of dissolved gases in groundwater samples from samples in fracture zones between 130 and 990 ft bls in the Laporte test hole are given in the Table A3. Relative concentrations are reported as mole percent of gas in the headspace extracted from water for 10 hydrocarbon gases (C_1 to C_6 alkanes and associated isomers) and six nonhydrocarbon gases (argon, oxygen, carbon dioxide, carbon monoxide, hydrogen, and nitrogen). The concentrations of methane, ethane, and ethene dissolved in water were quantified and reported as milligrams per liter.

Methane concentrations from fracture zones in the Huntley Mountain Formation at shallow and intermediate depths (130 to 425 ft bls) were either below detection or present at only trace concentrations less than 0.002 mg/L. Neither ethane nor propane were detected at these depths. Methane concentrations were elevated (14 mg/L) in the freshwater sample collected from fracture zones in the Catskill Formation at 637 to 644 ft bls and in the moderately saline sample from 990 ft bls (120 mg/L). Concentrations of ethane were much smaller—0.14 mg/L and 8.0 mg/L—from the fracture zone at 637 to 644 ft and the sample at 990 ft bls, respectively. Propane, isobutene, normal butane, and isopentane were detected in at least one sample, but the dissolved concentrations of those gases in water were not quantified. The ratio of the concentration of methane (C_1) to the sum of the higher chain hydrocarbon gases (C_2 to C_6) in mole percent was 192 for the sample from fractures at 637 to 644 ft bls and 27 for the sample collected 990 ft bls (Figure 31). Ratios less than 100 (Osborn and others, 2011) or 1,000 (Révész and others, 2012) have been used to typify methane of thermogenic origin.

The isotopic analyses of groundwater samples from the isolated fracture zone at 637–744 ft bls and the point sample at 990 ft bls in the open test hole are listed in Table A4. Stable isotope ratios were determined for $\delta^{13}C$ (carbon-13) in methane, ethane, propane, and dissolved carbon dioxide; δD (deuterium) in methane and water; and $\delta^{18}O$ (oxygen-18) in water. The $\delta^{13}C$ (methane) was -37.17 and -34.81 per mil and δD(methane) was -192.9 and -194.6 per mil for samples collected at the fracture zone at 637–644 ft and point sample at 990 ft bls respectively. The values are characteristic of gases with a thermogenic origin (Figure 32).

The $\delta^{13}C$ (ethane) was -36.1 per mil for the sample from 637–644 ft bls and -37.08 for the sample from 990 ft bls. The $\delta^{13}C$ value for methane from 640 ft bls was more depleted in ^{13}C than for ethane (larger negative values), which is characteristic of gases from the upper Devonian formations (Baldassare and others, 2014). However, the reverse is true for the sample from 990 ft bls—the value for ethane is more depleted in ^{13}C than the sample for methane. This reversal is commonly seen in deeper gases from the middle Devonian strata, including Marcellus Formation, but this sample documents an occurrence at an upland setting at a depth of 990 ft bls in the upper Devonian Catskill Formation.

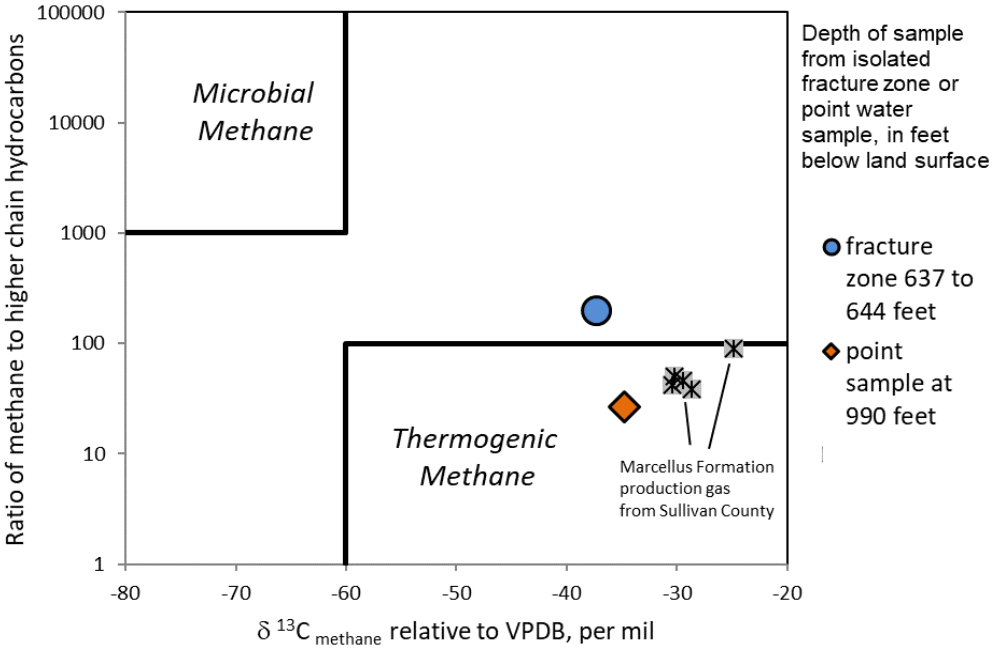

Figure 31. Bernard plot showing the relation between $\delta^{13}C$ of methane and the ratio of methane to the higher chain hydrocarbon gases (C2 to C6) in groundwater samples from 640 and 990 ft bls in the Laporte test hole, Sullivan County, Pa. Marcellus Formation production-gas data from gas wells in Sullivan County are from Reese and others (2013, table 7).

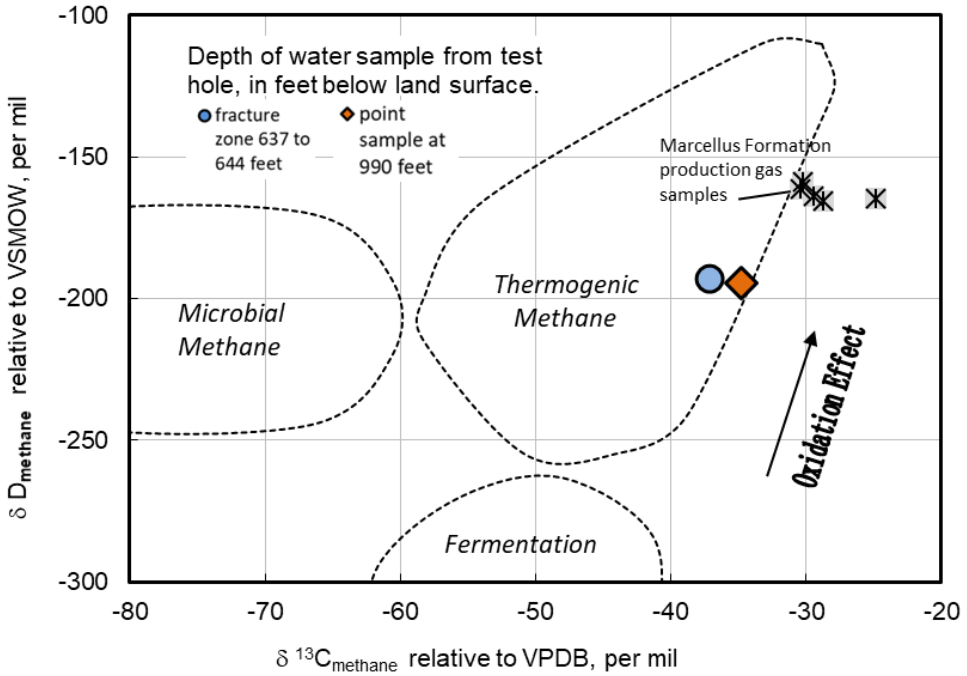

Figure 32. Stable carbon and hydrogen isotopic ratios for methane in water samples from the isolated fracture zone at 637 to 644 ft and point sample at 990 ft bls in the Laporte test hole, Sullivan County, Pa. Marcellus Formation production-gas data from gas wells in Sullivan County are from Reese and others (2013, table 7). Thermogenic, microbial, and fermentation fields are from Breen and others (2007, figure 19), which was modified from Coleman and others (1993).

Isotopic values for water (δD_{H2O} and $\delta^{18}O_{H2O}$) were analyzed for the groundwater samples in the Laporte test hole and compared to the local meteoric water line (Kendall and Coplen, 2001). The results of the analyses put the samples on the local meteoric water line, near the mean composition of precipitation sampled at Penn State (Figure 33) indicating that the groundwater probably recharged during post-glacial times. The isotopic composition is substantially different than waters from brines from oil and gas wells in western Pennsylvania reported by Dresel and Rose (2010, Table 7).

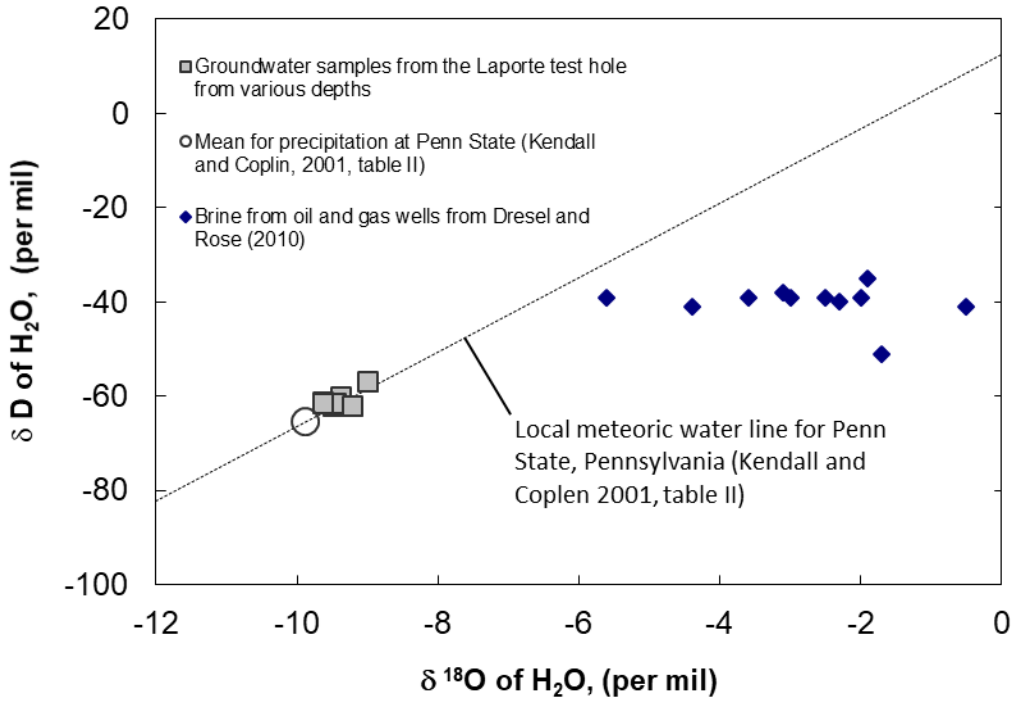

Figure 33. Stable isotopic composition of oxygen and hydrogen of water for seven groundwater samples from 160 to 990 ft bls from the Laporte test hole, Sullivan County, Pa., compared to precipitation sampled at State College, Pa., and to brines from oil and gas wells in western Pennsylvania from Dresel and Rose (2010).

Strontium isotopes ($^{87}Sr/^{86}Sr$) were analyzed for the highly saline sample collected at 990 ft bls that represents water entering the test hole from a fracture in the Upper Devonian Catskill Formation at 1,003 ft bls. The $^{87}Sr/^{86}Sr$ ratio of the sample was 0.71220, similar to the range of 0.71000–0.71212 reported for the Marcellus Formation brines by Warner and others (2012) in a study that used $^{87}Sr/^{86}Sr$ ratios to distinguish waters that might have mixed with Middle Devonian Marcellus Formation brines. The similarity of $^{87}Sr/^{86}Sr$ in the sample from Upper Devonian rocks in the Laporte test hole to Marcellus Formation brines illustrates the ambiguity in applying $^{87}Sr/^{86}Sr$ ratios to determine the source of brine.

ACTIVE GROUNDWATER FLOW AND DEPTH OF FRESH AND SALINE WATER

The 1,400-foot-deep Laporte test hole is in a broad, upland setting at the headwaters of the Loyalsock Creek watershed. In this setting near the watershed divide, groundwater moves laterally and downward through fractured sandstone and siltstone. A petrophysical log analysis by use of Archie's Equation indicates the transition from freshwater to saline water occurs between 450 to 900 ft bls (Figure 26). Water samples from isolated fracture zones at 130–135, 180, 267–275, and 425 ft bls are low-dissolved-solids, calcium-bicarbonate type freshwaters from sandstones in the Huntley Mountain Formation, verifying the occurrence of freshwater above 450 ft bls. Water sampled from a deeper fractured zone at 637–644 ft bls in the Catskill Formation is slightly saline sodium-bicarbonate-chloride type water. The relative increase in sodium and chloride concentrations in water from 637–644 ft bls, compared to samples from shallower zones, indicates that the fracture zone is probably in the lower, less active part of the groundwater flow system. Below 644 ft bls, few fractures are encountered, the temperature log approaches the geothermal gradient, fluid movement within the hole is very slow, and the hydraulic head equilibrates slowly when isolated by packers, all of which signify that there is minimal fracture transmissivity and little active flow below this depth. A low-permeability fracture penetrated at 1,003 ft bls in the Catskill Formation yields saline water. Saline water sampled at 990 ft bls has similar chemical characteristics to brines reported by Dresel and Rose (2010) that have been diluted by mixing with fresh water, and methane samples have isotopic signatures characteristic of thermogenic gases from Devonian rocks. The presence of thermogenic methane gas with the saline water at 990 ft bls in this upland setting is indicative of rocks that are not being flushed at that depth by active circulation of fresh water. Thus, it is likely that most active fresh groundwater flow occurs above 650 ft and that there is minimal flow below 900 ft bls at this upland location. Saline water would be expected below 900 ft bls. This is about the same as the depth of active groundwater flow found for the 1,664-ft-deep test hole in Bradford County and 1,513-ft-deep test hole in Tioga County (Risser and others, 2013; Williams and others, 2015).

A depth of saline water at 900 ft bls would be below the altitude of streams and ponds within about 3 to 5 miles from the test hole that act as drains from the local groundwater system, including Loyalsock Creek due north of the test hole (Figure 34). The lowest potential drain for the upland setting is at the mouth of Loyalsock Creek where it joins the West Branch Susquehanna River at an altitude of about 500 ft asl, which is about 930 ft deeper than the probable occurrence of saline water in the test hole.

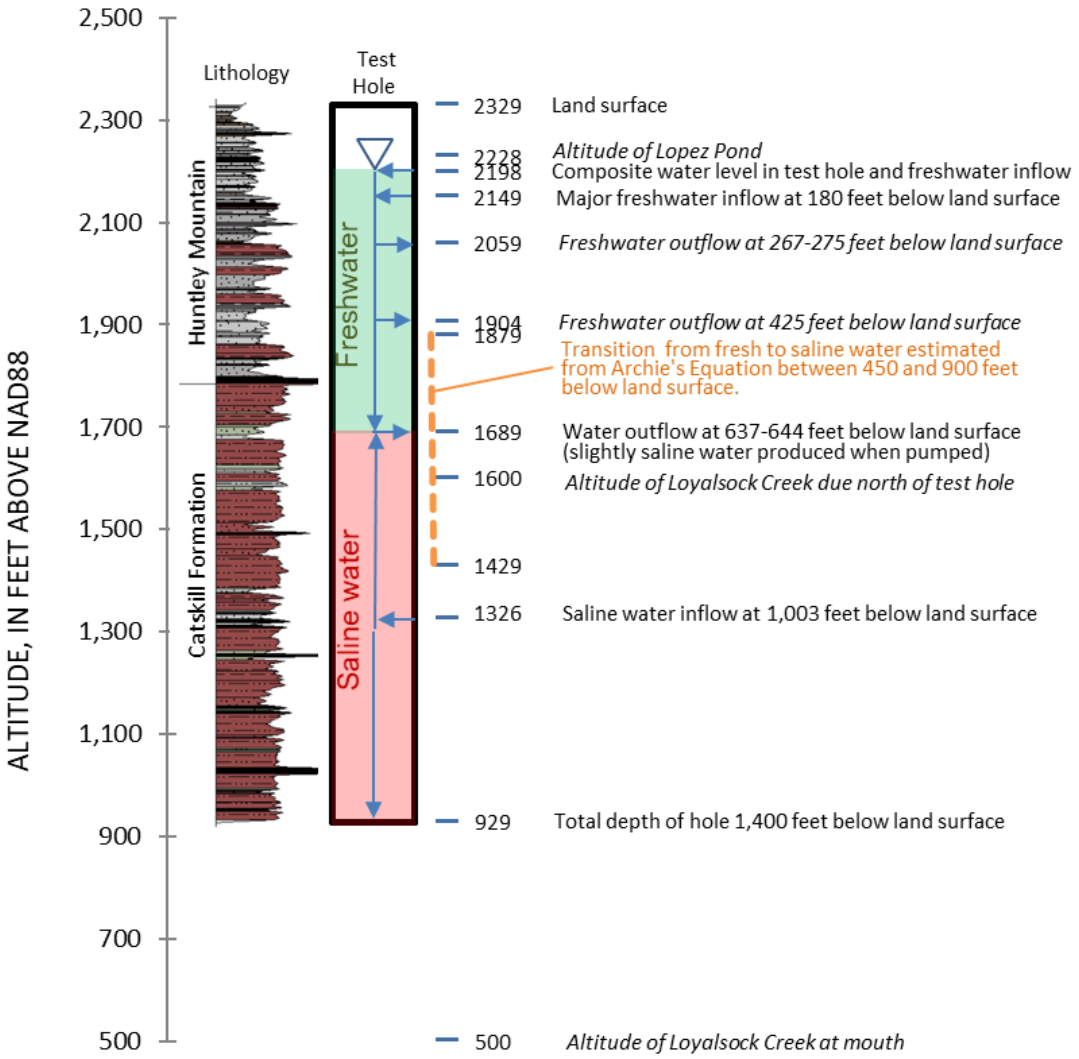

Green and red shadings in test hole represent parts of open hole being filled by fresh and saline water inflows, respectively. Arrows indicate fluid movement under ambient conditions in the open hole. Key to lithology symbols is on pages ix-xi.

Figure 34. Schematic diagram showing direction of ambient fluid movement and altitudes of water-bearing zones, and stream drainage in the vicinity of the Laporte test hole, Sullivan County, Pa.

SUMMARY

This report presents the results of a study to characterize the geohydrology and water quality of the Laporte test hole in Sullivan County, Pennsylvania, by an integrated analysis of measurements made during drilling, geophysical logging, and specific-depth groundwater sampling. The stratigraphy of the fractured sedimentary bedrock penetrated by the test hole is described; fractures and water-bearing zones are identified; and the chemical characteristics of groundwater, including isotopic signatures of dissolved hydrocarbon gases, are analyzed. The test hole was drilled in 2013 primarily to provide detailed geologic information for mapping of the Laporte 7.5-minute quadrangle, but also as a cooperative study between the Pennsylvania Bureau of Geological Survey and the U.S. Geological Survey described in this report to investigate the depth and composition of fresh and saline groundwater in an area

of development of shale gas from the Marcellus Formation. Information about the depth of fresh groundwater could help gas operators protect groundwater resources. This is the third report on results of investigations of deep test holes in northern Pennsylvania. Results from a 1,513-ft-deep core hole in south-central Tioga County and a 1,664-ft-deep core hole in western Bradford County have been previously reported (Risser and others, 2013; Williams and others, 2015).

The Laporte test hole was drilled with air-hammer methods to a depth of 1,400 ft bls in an upland setting within the Loyalsock Creek watershed, near its divide with Muncy Creek. The hole was completed with 8.75-inch steel casing from 0 to 40 ft bls, with an 8-inch open hole from 40 to 500 ft bls and 6-inch open hole from 500 to 1,400 ft. The test hole penetrated unconsolidated bedrock residuum and till to a depth of 8.5 ft bls, the Huntley Mountain Formation of Mississippian and Devonian age to a depth of 540 ft bls, and the Catskill Formation of Devonian age from 540 to 1,400 ft bls. Rock cuttings collected during drilling showed that the Huntley Mountain Formation consists of gray sandstone with minor gray shales and red-bed intervals of claystone and siltstone; the Catskill Formation has more abundant and thicker red-bed intervals than the Huntley Mountain Formation that are chiefly grayish-red siltstone and claystone with brownish-gray sandstone. Cuttings are stored in the BGS core library in Middletown, Pennsylvania, and are available for examination upon request.

The distribution and orientation of fractures, bedding features, and breakouts were determined by analyzing the optical televiewer log, modified by information from the acoustic televiewer and video logs. Bedding features penetrated by the test hole were characterized as planar with noticeable crossbedding. Bedding was estimated to have a strike of 243 degrees and dip about 4 degrees to the northwest, consistent with its location on the north limb of the Muncy Creek anticline. Fractures were commonly penetrated from 50 to 200 ft bls (density of about 21 fractures per 50 ft of hole), then generally decreased with depth to the bottom of the hole except for a notable increase at the highly fractured zone from 637 to 644 ft. Below 644 ft bls there is a marked decrease in fracture density to about 1.6 per 50 ft of hole. About 80 percent of the fractures penetrated by the test hole were low-angle features dipping less than 20 degrees in all directions. Breakouts, formed by spalling of rock from the test-hole wall, were discontinuously present from 756 to 938 ft bls, indicating that the direction of maximum modern-day horizontal stress was at an azimuth of about 70 degrees.

The test hole penetrated multiple water-bearing zones with differing hydraulic heads and transmissivity. The depths of water-bearing zones were identified by measurements of water discharge during drilling and analysis of geophysical logs. Six major water-bearing zones associated with single or multiple fractures were identified at depths of 130–135, 180, 267–275, 425, 637–644, and 1,003 ft bls. Under ambient conditions, freshwater from sandstones in the Huntley Mountain Formation enters the test hole from fractures at 130–135, 180, 267–275, and 425 ft bls, moves downward, and exits the hole at a transmissive fracture zone from 637–644 ft bls in the Catskill Formation. When pumped at 16.2 gal/min, most of the water was contributed from the fracture at 180 ft bls. The hydraulic heads in the water-bearing fracture zones at 425 and 637–644 ft bls were about 100 ft lower than hydraulic heads in shallow water-bearing zones at 180 ft bls and above. A time-series of specific-conductance logs indicated seepage of saline water into the test hole from a low-permeability fracture penetrated at 1,003 ft bls in the Catskill Formation, and image logs showed streaks on the

test-hole wall indicating inflow at that depth, and from several bedding-plane fractures at about 958 and 989 ft bls.

Transmissivity, estimated from analysis of the specific-capacity data and flowmeter logs, was about 850 ft^2/d for the entire open hole, and about 60 percent of the transmissivity was contributed from the fracture zone at 180 ft bls. Below 644 ft bls, few fractures were penetrated by the test hole and the temperature log approaches the geothermal gradient indicating that there is minimal fracture transmissivity and active flow below this depth.

Specific-depth samples of groundwater were collected from this upland test hole by isolating the water-bearing fractures at 130–135, 180, 267-275, 425, 637–644 ft bls with packers. The dissolved-solids concentrations of water samples collected from isolated intervals indicated that all samples collected at depths down to 425 ft bls are fresh water with dissolved solids less than 1,000 mg/L. The dissolved-solids concentration of the water sample from fractures 637–644 ft bls was probably affected by leakage of water from above the packer. However, the specific conductance of the water blown to the surface from that depth during drilling indicates that the water is slightly saline, with a dissolved-solids concentration of about 1,100 mg/L. A groundwater sample was collected with a wireline point sampler at 990 ft bls; the dissolved-solids concentration of that sample was 19,900 mg/L when sampled on July 28, 2014, which is highly saline. The saline water sampled at 990 ft bls had a chemical composition similar to Appalachian Basin brines that had been diluted with fresh water. Predominant ions in the saline water were sodium, chloride, and calcium. The trace elements strontium, bromide, barium, lithium, and molybdenum were all more than 5,000 times greater than in freshwater samples from 130–135 or 180 ft bls. The major-ion chemistry of the sample from fractures at 637–644 ft bls differed from the waters in the test hole above and below. The sample was a sodium-bicarbonate-chloride water, but it is not a mixture of the shallow calcium-bicarbonate water with the deep sodium-chloride water. Rather, it probably evolved when recharge water flowed downward through shales in the Catskill Formation, exchanging calcium ions for sodium ions, then mixed with saline pore fluids. However, some leakage through the straddle-packer seal during pumping could have affected this sample chemistry.

Methane concentrations in groundwater samples were 14 mg/L in the freshwater sample collected at 640 ft bls and 120 mg/L in the saline sample from 990 ft. The concentration ratios of methane to higher-chain hydrocarbon gases and isotopic ratios of $^{13}C/^{12}C$ and $^{2}H/^{1}H$ of methane indicated that the gases are likely of thermogenic origin. The $^{13}C/^{12}C$ of methane was less negative (-34.81 per mil) than the $^{13}C/^{12}C$ of ethane (-37.1 per mil) in the gas sample collected from 990 ft bls, which is the reverse of what is normally expected in gases from the Catskill Formation in Pennsylvania. This isotopic reversal is generally found in gases from rocks older than the Catskill Formation, so recognition of this occurrence could be useful in the interpretation of isotopic results for identifying gas origin.

A petrophysical log analysis using estimates of formation water resistivity from Archie's Equation indicated an apparent transition from fresh to saline water in the sandstones occurs between 450 to 900 ft bls, with saline water indicated below 900 ft bls. This range was consistent with the distribution of freshwater-bearing zones sampled from 130 to 425 ft bls, transitional water-bearing zone at 637–644 ft bls, and saline water-bearing zone at 1,003 ft bls. A depth of saline water at 900 ft bls would be below the altitude of the streams and ponds

that act as drains for the local groundwater system and is just below the altitude of the Loyalsock Creek due north of the test hole. A depth of saline water at 900 ft bls would be below the altitude of the streams and ponds within about 3 to 5 miles from the test hole that act as drains for the local groundwater system. The lowest potential drain for the upland setting is the mouth of Loyalsock Creek where it enters the West Branch Susquehanna River at an altitude of about 500 ft asl, which is about 930 ft below the probable depth of saline water in the test hole.

ACKNOWLEDGMENTS

The authors acknowledge the Pennsylvania Game Commission for permission to drill the Laporte test hole on State Game Land 13. Alton Anderson, Randall Conger, and Philip Bird of the USGS collected the geophysical logs and borehole videos and assisted with groundwater sampling. Colleague reviews of the report were provided by William Kappel, Philip Bird, and Jeffrey Chaplin of USGS.

REFERENCES CITED

Alley, W. M., 2003, Desalination of ground water—Earth science perspectives: U.S. Geological Survey Fact Sheet 075–03, 4 p.

Archie, G. E., 1942, The electrical resistivity log as an aid in determining some reservoir characteristics: American Institute of Mining, Metallurgical, and Petroleum Engineers Transactions, v. 146, p. 54–62.

Baldassare, F. J., McCaffrey, M. A., and Harper, J. A., 2014, A geochemical context for stray gas investigations in the northern Appalachian Basin—Implications of analyses of natural gases from Neogene-through Devonian-age strata: AAPG Bulletin, v. 98, no. 2, p. 341–372.

Breen, K. J., Révész, Kinga, Baldassare, F. J., and McAuley, S. D., 2007, Natural gases in ground water near Tioga Junction, Tioga County, north-central Pennsylvania—Occurrence and use of isotopes to determine origins, 2005: U.S. Geological Survey Scientific Investigations Report 2007–5085, 65 p. Portable Document Format (PDF) [http://pubs.usgs.gov/sir/2007/5085/pdf/ sir2007-5085.pdf, accessed April 11, 2014].

Coleman, D. D., Liu, C. L., Hackley, K. C., and Benson, L. J., 1993, Identification of landfill methane using carbon and hydrogen isotope analysis, *in* Proceedings, Sixteenth International Madison Waste Conference: Municipal & Industrial Waste, September 22–23, 1993: Department of Engineering Professional Development, University of Wisconsin-Madison, p. 303–314.

Commonwealth of Pennsylvania, 2014, Pennsylvania Code, Title 25, Environmental Protection, Chapter 93, Water Quality Standards, Section 7, Specific Water Quality Criteria, [December 29, 2014, http://www.pacodeandbulletin.gov/Display/pacode?file=/secure/pacode/data/025/chapter93/s93.7.html&d=reduce].

Cooper, H. H., and Jacob, C. E., 1946, A generalized graphical method for evaluating formation constants and summarizing well-field history, American Geophysical Union Transactions, v. 27, p. 526–534.

Davis, S. N., Whittemore, D. O., and Fabryka-Martin, 1998, Uses of chloride/bromide ratios in studies of potable water: Ground Water, v. 36, no 2, p. 338–350.

Day-Lewis, F. D., Johnson, C. D., Paillet, F. L., and Halford, K. J., 2011, A computer program for flow-log analysis of single holes (FLASH): Ground Water, v. 49, p. 926–931.

Dresel, P. E., and Rose, A. W., 2010, Chemistry and origin of oil and gas well brines in western Pennsylvania: Pennsylvania Geological Survey, 4th ser., Open-File Report OFOG 10–01.0, 48 p. Portable Document Format (PDF).

Faill, R. T., compiler, 2011, Folds of Pennsylvania—GIS data and map: Pennsylvania Geological Survey, 4th ser., Open-File Report OFGG 11–01.1, 1 map, scale 1:500,000.

Hearst, J. R., and Nelson, P. H., 1985, Well logging for physical properties: New York, McGraw-Hill, 571 p.

Hess, A. E., 1982, A heat-pulse flowmeter for measuring low velocities in boreholes: U.S. Geological Survey Open-File Report 82–699, 44 p. Portable Document Format (PDF) [March 2013, https://pubs.er.usgs.gov/publication/ofr82699].

Johnson, C. D., 1996, Use of a borehole color video camera to identify lithologies, fractures, and borehole conditions in bedrock wells in the Mirror Lake Area, Grafton County, New Hampshire, *in* Morganwalp, D. W., and Aronson, D. A., eds., U.S. Geological Survey, Toxic Substance Hydrology Program Proceedings of the Technical Meeting, Colorado Springs, Colorado, September 20–24, 1993: U.S. Geological Survey Water-Resources Investigations Report 94–4015, v. 1, p. 89–94. Portable Document Format (PDF) [March 2013, http://pubs.usgs.gov/wri/1994/4015/report.pdf].

Jorgensen, D. G., and Petricola, Mario, 1994, Petrophysical analysis of geophysical logs of the National Drilling Company—U.S. Geological Survey ground-water research project for Abu Dhabi Emirate, United Arab Emirates: U.S. Geological Survey Water-Supply Paper 2417, 35 p.

Kelley, D. R., 1969, A summary of major geophysical logging methods: Pennsylvania Geological Survey, 4th ser., Mineral Resource Report 61, 82 p.

Kendall, Carol, and Coplen, T. B., 2001, Distribution of oxygen-18 and deuterium in river waters across the United States: Hydrological Processes, v. 15, p. 1363–1393.

Keys, W. S., 1990, Borehole geophysics applied to ground-water investigations: U.S. Geological Survey Techniques of Water-Resources Investigations, book 2, chap. E2, 150 p.

Mullaney, J. R., Lorenz, D. L., and Arntson, A. D., 2009, Chloride in groundwater and surface water in areas underlain by the glacial aquifer system, northern United States: U.S. Geological Survey Scientific Investigations Report 2009–5086, 41 p.

Munsell, 2009, Geological rock-color chart, Munsell Color, 4300 44th St., Grand Rapids, Mich.

Osborn, S. G., Vengosh, Avner, Warner, N. R., and Jackson, R. B., 2011, Methane contamination of drinking water accompanying gas-well drilling and hydraulic fracturing: National Academy of Sciences USA Proceedings, v. 108, p. 8172–8176.

Paillet, F. L., 1998, Flow modeling and permeability estimation using borehole logs in heterogeneous fractured formations: Water Resources Research, v. 34, no. 5, p. 997–1010.

Paillet, F. L., 2000, A field technique for estimating aquifer parameters using flow log data: Ground Water, v. 38, no. 4, p. 510–521.

Paillet, F. L., Hess, A. E., Cheng, C. H., and Hardin, E. L., 1987, Characterization of fracture permeability with high-resolution vertical flow measurements during borehole pumping: Ground Water, v. 25, no. 1, p. 28–40.

Pennsylvania Department of Environmental Protection, 2006, Maximum contaminant levels (MCLs): Bureau of Safe Drinking Water, Division of Drinking Water Management [December 29, 2014, http://files.dep.state.pa.us/Water/BSDW/DrinkingWaterManagement/PrivateWaterWells/PA_MCLs_06.pdf].

Pennsylvania Department of Environmental Protection, 2013, PA Oil and Gas Mapping: Office of Oil and Gas Management, Interactive Map, [July 12, 2013, http://www.depgis.state.pa.us/PaOilAndGasMapping/].

Reese, S. O., Neboga, V. V., Pelepko, Seth, and others, 2014, Groundwater and petroleum resources of Sullivan County, Pennsylvania: Pennsylvania Geological Survey, 4th ser., Water Resource Report 71, 99 p., 6 pls., plus 27 p. appendix.

Rider, M. H., and Kennedy, Martin, 2011, The geological interpretation of well logs (3rd ed.): Glascow, Rider-French Consulting Limited, 432 p.

Risser, D. W., Williams, J. H., Hand, K. L., and others, 2013, Geohydrologic and water-quality characterization of a fractured-bedrock test hole in an area of Marcellus shale gas development, Bradford County, Pennsylvania: Pennsylvania Geological Survey, 4th ser., Open-File Report OFMI 13–01.1, 49 p., 4 appendices.

Senior, L. A., Cravotta, C.A., III, and Sloto, R. A., 2017, Baseline assessment of groundwater quality in Wayne County, Pennsylvania, 2014, ver. 1.1: U.S. Geological Survey Scientific Investigations Report 2016–5073, 136 p. [March 2017, http://dx.doi.org/10.3133/sir20165073].

Theis, C. V., Brown, R. H., and Meyer, R. R., 1963, Estimating the transmissibility of aquifers from the specific capacity of wells, *in* Bentall, Ray, compiler, Methods of determining permeability, transmissibility and drawdown: U. S. Geological Survey Water-Supply Paper 1536–I, p. 331–340.

U.S. Environmental Protection Agency, 2009, National primary drinking water regulations [and] national secondary drinking water regulations: EPA 816-F-09-004, 6 p. Portable Document Format (PDF) [April 25, 2014, http://www.epa.gov/safewater/consumer/pdf/mcl.pdf].

U.S. Geological Survey, [2019a], STATEMAP—State Geologic Survey Mapping Component of the National Cooperative Geologic Mapping Program [February 24, 2019, https://www.usgs.gov/core-science-systems/national-cooperative-geologic-mapping-program/science/statemap-state-geologic?qt-science_center_objects=0#qt-science_center_objects].

_____ [2019b], USGS GeoLog Locator: U.S. Geological Survey [February 29, 2019, https://webapps.usgs.gov/geologlocator/#!/].

_____ [2019c], Water basics glossary: U.S. Geological Survey [February 24, 2019, https://water.usgs.gov/water-basics_glossary.html].

Warner, N. R., Jackson, R. B., Darrah, T. H., and others, 2012, Geochemical evidence for possible natural migration of Marcellus Formation brine to shallow aquifers in Pennsylvania: National Academy of Sciences USA Proceedings, v. 109, p. 11961–11966.

Wilde, F. D., Radtke, D. B., Gibs, Jacob, and Iwatsubo, R. T., eds., 2002–2009, Processing of water samples (version 2.2, with updates through 2009): U.S. Geological Survey Techniques of Water-Resources Investigations, book 9, chap. A5, 122 p. Portable Document Format (PDF) [October 2, 2012, http://pubs.water.usgs.gov/twri9A5/].

Williams, J. H., and Johnson, C. D., 2004, Acoustic and optical borehole-wall imaging for fractured-rock aquifer studies: Journal of Applied Geophysics, v. 55, iss. 1–2, p. 151–159. Portable Document Format (PDF) [http://water.usgs.gov/ogw/bgas/publications/JAG_2004/JAG_2004.pdf].

Williams, J. H., Risser, D. W., and Dodge, C. H., 2015, Geohydrologic and water-quality characterization of a fractured-bedrock test hole in an area of Marcellus shale gas development, Tioga County, Pennsylvania: Pennsylvania Geological Survey, 4th ser., Open-File Report OFMI 15–24.0, 44 p. plus supplemental information.

Young, S. C., and Pearson, H. S., 1995, The electromagnetic borehole flowmeter—Description and applications: Ground Water Monitoring and Remediation, v. 15, no. 4, p. 138–146.

Zoback, M. L., and Zoback, Mark, 1980, State of stress in the conterminous United States: Journal of Geophysical Research, v. 85, no. B11, p. 6113–6156.